

**A REMOTE-SENSING BASED INVESTIGATION ON THE IMPACTS OF CANOPY
HEIGHT DIFFERENCES ON MICROCLIMATE IN A BURNED FOREST**

by

Sarah Smith-Tripp

B.A., Wellesley College, 2019

A THESIS SUBMITTED IN PARTIAL FULFILLMENT OF
THE REQUIREMENTS FOR THE DEGREE OF

MASTER OF SCIENCE

in

THE FACULTY OF GRADUATE AND POSTDOCTORAL STUDIES
(Geography)

THE UNIVERSITY OF BRITISH COLUMBIA

(Vancouver)

July 2021

© Sarah Smith-Tripp, 2021

The following individuals certify that they have read, and recommend to the Faculty of Graduate and Postdoctoral Studies for acceptance, a thesis entitled:

A remote-sensing based investigation on the impacts of canopy height differences on microclimate in a burned forest

submitted by Sarah Smith-Tripp in partial fulfillment of the requirements for

the degree of Master of Science

in Geography

Examining Committee:

Dr. Naomi Schwartz, Assistant Professor, Department of Geography, UBC

Supervisor

Dr. Bianca Eskelson, Associate Professor, Department of Forest Resources Management, UBC

Supervisory Committee Member

Dr. Nicholas Coops, Professor, Department of Forest Resources Management, UBC

Supervisory Committee Member

Dr. Dan Moore, Professor, Department of Geography, UBC

Additional Examiner

Abstract

Forested canopies buffer seedlings from extreme climate conditions, but whether burned forests maintain this buffering capacity is not well understood. Previously, modeling the impact of a forest canopy on microclimate conditions was difficult because microclimate dynamics occur over fine-spatial scales. Inputs for microclimate modeling thus require high-resolution data. New technology like remotely piloted aircraft (RPAs) and low-cost microclimate sensors allow for a rapid expansion in microclimate modeling. My research capitalized on technological advancements to produce accurate and high spatial resolution descriptions of forest canopies to explain microclimate variation in a sub-boreal forest impacted by variable fire severity. To address a need for standardized microclimate modeling methods, I compare correlations of microclimate metrics to canopy height summarized at different scales of spatial buffers. Results demonstrate that the optimum scale for summarizing canopy height is dependent on the variable of interest – soil moisture is better explained by smaller buffers and temperature by moderately sized spatial buffers. I use these buffers to model the relationship between canopy height and microclimate. I found that growing season near-surface, surface, and soil temperatures increased linearly with decreasing canopy height and cover. Of near-ground temperatures, soil temperature showed the strongest correlation with canopy height, where a reduction of 10 m in canopy height was associated with a 1.5 °C increase in mean growing-season soil temperature. There was a weak negative relationship between canopy height and soil moisture, which I attribute to confounding effects of high evaporation in burned canopies and high transpiration in unburned canopies. My findings underline the importance of including canopy in post-disturbance microclimate models, as differences in soil temperature can impact the distribution of seedlings and other species.

Lay summary

Forest canopies protect near-ground environments from climate extremes by cooling in extreme hot and warming in extreme cold; however, after forest fires, near-ground environments may lose protection from the canopy. Globally, accurate models of near-ground environments are not widely available. Production of these models requires knowing the relationship between burned forest canopies and near-ground environments. This thesis combines high-quality remotely piloted aircraft (RPAs) canopy height data and near-ground temperature and moisture measurements to model the relationship between the ground and a burned forest canopy. Results indicate that taller canopies decrease temperatures, but the degree of cooling varies throughout the season. Using high-quality remote sensing data, I found soils beneath tall canopies were drier than those with shorter canopies, but differences in moisture content between tall and short canopies were generally small. Thus, climate modelers should consider the relatively weak influence of burned canopies on soil moisture and a dynamic relationship between tree canopy and temperature throughout the growing season.

Preface

The microclimate study in Alex Fraser Research Forest was developed in collaboration with my supervisor, Dr. Naomi Schwartz. I selected the field site and developed a sampling strategy with feedback from Professors Naomi Schwartz, Bianca Eskelson, and Nicholas Coops. I also gained permission to place study sites within an existing research project of Professor Suzanne Simard. I was responsible for the COVID-19 safety plan, data collection, fieldwork logistics, equipment acquisition, and data processing with the help of several field assistants. I worked principally with Rithikha Rajamohan to set up sites, collect field data, and fly remotely piloted aircraft (RPA). Professor Schwartz, Elise Pletcher, and Tony Zhang also assisted with field data collection. I processed all field data and submitted my dataset to the SoilTemp database, a global repository for near-surface climate data. Research equipment was provided by Professors Schwartz, Coops, and Smukler. I was responsible for calibrating all field equipment before use. Models, including canopy height and linear models, were developed with input from Professors Schwartz, Coops, and Eskelson. This thesis is the original, unpublished work of the author, Sarah Smith-Tripp. All writing, figures, and tables are my work. Reviews were kindly offered by Professors Schwartz, Eskelson, and Coops, as well as Elise Pletcher. Chapter 3 is planned for submission to an meteorology or remote sensing journal.

This work was also presented as:

Smith-Tripp, S., Coops, N., Eskelson, B. I., Schwartz, N. B., (2021) T-07: Integrating Remote Sensing as a Tool to Model Canopy Influence on Microclimate Variation in Disturbed Forests. *IALE-NA Annual Meeting*. Reno, NV (remote). April 12 – 15. Presentation

Table of Contents

Abstract.....	iii
Lay summary.....	iv
Preface.....	v
Table of Contents	vi
List of Tables	x
List of Figures.....	xi
List of Supplementary Material	xiv
List of Abbreviations	xv
Acknowledgements	xvi
Dedication	xvii
Chapter 1: Introduction	1
1.1 Research objectives.....	4
Chapter 2: Literature review of variables known to influence microclimate	6
2.1 Major microclimate drivers.....	6
2.1.1 Topography	6
2.1.2 Soil	8
2.1.3 Understory structure.....	9
2.1.4 Tree canopy.....	10
2.2 Differences in microclimate dynamics following tree canopy disturbance	12
2.3 The use of remote sensing to enhance microclimate understanding.....	17
2.3.1 Remotely piloted aircraft for high-resolution measurements of forest structure ..	19
2.4 Conclusions from review	21

Chapter 3: Canopy height effects on the growing season and monthly microclimate in a burned forest of British Columbia, Canada	22
3.1 Introduction.....	22
3.2 Methods.....	25
3.2.1 Study area and forest plots	25
3.2.2 Datalogger locations and data compilation.....	25
3.2.3 LiDAR-derived aspect data.....	27
3.2.4 Remotely piloted aircraft data and canopy height modeling	28
3.2.5 Analyses.....	31
3.2.5.1 Research question 1: Linear models to assess the scale of spatial buffer for canopy influence	31
3.2.5.2 Research question 2: Mixed linear models to determine the impact of canopy height on microclimate variables of interest.....	31
3.3 Results.....	34
3.3.1.1 Means (growing season and monthly) and mean daily ranges of microclimate variables	34
3.3.2 Research question (1): Linear correlation between canopy height and mean temperature and soil moisture differs as a function of spatial buffer	37
3.3.3 Question 2a : Canopy height consistently explains growing season microclimate	39
3.3.4 Question 2b: The impact of canopy height on monthly mean microclimate differs throughout the season	42
3.4 Discussion.....	43

3.4.1	Tree canopy height explains microclimate temperatures over other known microclimate drivers	44
3.4.2	The impact of tree canopy on microclimate variables in the context of successful regeneration.....	46
3.4.3	Scale of spatial buffer necessary for microclimate modeling differs by microclimate variable, temperature, or soil moisture	47
3.4.4	Improving microclimate modeling in disturbed environments using remote sensing	48
Chapter 4: Conclusions		50
4.1	Overarching goal of research: relationship between disturbed canopy and microclimate	50
4.2	Importance of research and key findings	51
4.3	Limitations of research	53
4.3.1	Assumptions of the study design	53
4.3.2	Measurement error	55
4.4	Future work.....	56
4.4.1	Analyses utilizing the thesis dataset	56
4.4.2	Expansion of microclimate research at a global scale	57
References		58
Appendices.....		68
Appendix A RPA flights and 3D point cloud development		68
Appendix B Microclimate data cleaning		69
B.1	Rolling mean standard deviation in soil temperature	69

B.2	Microclimate data included in analyses	70
Appendix C	Canopy height models and verification	72
C.1	Canopy height models.....	72
C.2	Canopy verification plots	73
C.3	Accuracy of DAP model compared to field measured sites	74
Appendix D	Correlation coefficients for canopy attributes and model predictors	77
D.1	Correlation between canopy height and canopy cover	77
D.2	Correlation between model fixed effects	77
Appendix E	Estimated parameters of monthly models for all explanatory variables.....	78
Appendix F	Field collected data	79
F.1	Vegetation and leaf litter data	79
F.2	Soil data	80
F.3	Leaf area index data	83

List of Tables

Table 2.1 Selection of microclimate studies in disturbed forests. Studies quantify the impact of an overstory (canopy height, density, cover) gradient on microclimate dynamics. Studies that consider natural disturbances are colored in grey.....	15
Table 2.2 Studies comparing spatial resolution used to build either predictive or explanatory microclimate models. Studies limited to those that either downscaled regional climate models or compared regional climate models to in-situ measurements.	19
Table 3.1 Summary statistics of growing season microclimate data and explanatory variables: canopy height, elevation, and aspect. Mean growing season values are the mean for the growing season. The mean growing season range is the mean of the daily range in microclimate variables. Aspect is presented in degrees, but models used a converted aspect (Eq 1).	35
Table 3.2 Optimal models for mean growing season microclimate variables. The full model included canopy height, elevation, aspect, and plot as a random effect (Eq. 2). * Notes that the microclimate variable was log-transformed to meet model assumptions. Std. Dev is the standard deviation.....	40
Table S1 Details of equipment and flight planning for RPA image acquisition.	68
Table S2 Point cloud accuracy for photo-alignment (RTK photo alignment), LiDAR ICP alignment and orthophoto rectification.....	68
Table S3 Pearson's correlation coefficient for fixed effects used in mixed linear models. Correlation coefficients are included for canopy calculated at the 2 m (used to model soil moisture) and 15 m (used to model soil temperature) radius.....	77

List of Figures

Figure 2.1 Schematic water flow rates in a system at different slopes with consistent soil composition. System water flow rates determine site-level soil moisture. Lateral flows are shown in the red-box subset. The size of the arrows on horizontal flows denotes relative flow rates.
Note: There is no consideration of evapotranspiration. 7

Figure 2.2 Schematic of water flow on a vegetated surface. Arrows show the approximate scale of relationships. 12

Figure 3.1 Orthophotos for four flight areas. Datalogger locations are noted in orange, and forest canopy verification plots in blue. Numbers correspond to forest plots. There are 9 dataloggers per forest plot. The inset map shows the 2009 LiDAR DEM and the 2017 fire boundary. 30

Figure 3.2 (A-C) Mean monthly temperatures and (D) weekly means of soil moisture for dataloggers. The dark line is the mean soil moisture for the AFRF field site, and the grey band is the standard deviation. Note: the high value in mean soil moisture is a datalogger in a wet location where equipment was removed early in the season. The equipment was replaced in July. 36

Figure 3.3 Model R^2 for microclimate growing season means at 2, 5, 10, 15, and 20 m radii. Points are colored by model type: Soil – dark red, surface – red, Near-Surface – light red, Soil Moisture – blue. Note: these models do not include aspect and elevation included in later modeling 38

Figure 3.4 Mean growing season temperature and mean daily range as a function of canopy height. Temperatures for soil, surface, and near-surface are shown in different panels. Points are colored by forest plot. Lines show predictions of mixed effects models. *Notes that the

microclimate variable was log-transformed to meet model assumptions (including mean growing season soil moisture)..... 41

Figure 3.5 (A-D) Confidence interval and model estimate for canopy height to mean monthly microclimate variables (Near-Surface, Soil, Surface, and Soil Moisture). Points show model estimates for models fit to data by month. Bars are the 95% confidence intervals for the parameter estimate. Note: vertical scales differ by the panel. (E) Adjusted model R^2 for each monthly model. Color and shape align with microclimate variable. 43

Figure S1 Example from datalogger 66 of the 7-day mean of soil temperature daily standard deviation used to clip data. A large increase in the 7-day mean supports the datalogger 66 was removed on day 204..... 69

Figure S2 Soil Moisture, soil and surface temperatures included in analyses. Plot ID is noted on the vertical axis, and lines are colored by forest plot. Data were removed based on known issues with the data (the logger was pulled out of the ground) or erroneous data (unusually high or low values)..... 70

Figure S3 Near-Surface temperatures included in analyses. Plot ID is noted on the vertical axis, and lines are colored by forest plot. Data were removed based on known issues with the data (the solar shield was removed) or the data were erroneous (unusually high or low values). 71

Figure S4 Canopy height models for the field site. Each raster has a 10cm resolution, and the color scale is the same for all plots. Datalogger locations are noted in orange. Numbers are the plot locations. 72

Figure S5 Verification plots for canopy height models. Plots are labeled according to randomly assigned labels. Points are the distance from plot center. Tree height (m) is a gray scale of white to black and point size corresponds to diameter-at-breast-height (cm). 73

Figure S6 Comparison of DAP derived and field measured maximum and mean verification plot heights. The dotted line in S11B is the model result including the outlier data point (the triangle).
..... 75

Figure S7 Description of error introduced comparing high burn severity canopy height data to low burn severity canopy height data. Circles denote the plot area. Stem plot circles depict diameter-at-breast-height (cm) of measured stems. Height values are arbitrarily chosen to show differences in high and low burn severity canopy height rasters and field plot data. 76

Figure S8 Correlation between canopy cover and canopy height for radii used in microclimate modeling. Rho (ρ) is the spearman correlation of the two variables 77

Figure S9 Estimated parameter for fixed effects on mean microclimate variables averaged by month (Near-Surface, Soil, Surface, and Soil Moisture vol %). Points show estimated parameters, and surrounding lines are the 95% confidence intervals for parameters. Printed text values are the adjusted model R^2 . Note: vertical scales differ among panels. 78

Figure S10 Variability in litter depth and vegetation height. Points are average values for each datalogger. Distribution is based on all points (5 per datalogger). 80

Figure S11 Example soil core from plot six datalogger number four. Soil cores generally showed these three distinct layers, organic dominant (top), silty sand matrix (middle), and a silt matrix (base). 81

Figure S12 Soil samples from plot 4. Samples are combined cores from each datalogger. 82

Figure S13 Plot-level variability in bulk density (g/cm^3). Points show values derived for each plot 83

Figure S14 Leaf area index measurements for each datalogger. Points and boxes are colored by plot number. 84

List of Supplementary Material

CA_ST_data_complete.xlsx

CA_ST_MetaData_27-Nov-2020.csv

SoilTemp_MetaData_Details.pdf

List of Abbreviations

AFRF – Alex Fraser Research Forest

AIC – Akaike Information Criterion

ALS – Airborne laser scanning

BC – British Columbia

CHM – Canopy Height Model

DAP – Digital Aerial Photogrammetry

DBH – Diameter at breast height

DEM – Digital Elevation Model

dNBR – difference in Normalized Burn Ratio

DSM – Digital Surface Model

GCP – Ground Control Point

ICP – Iterative Closest Point

LAI – Leaf Area Index

LiDAR – Light detection and ranging

RMSE – Root Mean Square Error

RPA – Remotely Piloted Aircraft

RTK – Real-time Kinetic

SBS – Sub-boreal Spruce

Acknowledgements

I must first acknowledge this research was conducted on the traditional, ancestral, and unceded land of the traditional territory of the Northern Secwepemc te Qelmuw people. I am thankful to learn from this land. I also would like to thank my supervisor Dr. Naomi Schwartz for her constant support during my research process. The independence offered to build and implement my research project has empowered me as a researcher and scholar. I give a deeply heartfelt thank you to my committee members Dr. Bianca Eskelson and Dr. Nicholas Coops, for your support in completing my thesis and my degree. I thank Dr. Coops for my honorary lab position with the Integrated Remote Sensing Studio (IRSS). The knowledge and resources of Dr. Coops and IRSS labmates, particularly Jeremy Arkin, were crucial to this work's success. Thank you to Dr. Eskelson for providing theoretical background, statistical support for my fieldwork and analyses, and careful manuscript review.

To the other Schwartz lab members, Elise, Adrian, and Tony, thank you for being my sounding board through this process. I owe you many thanks. I thank my IRSS buds, Evan Muise, Cameron Cosgrove, Claire Armor, and Samuel Grubinger. Although much of our time was spent physically apart, you were always there to laugh when my graphs looked like nonsense. Finally, I thank Trevor and Jennifer Harris for listening on the good and long days.

I want to thank my family, particularly my sister, for surviving two weeks locked in a room with me. To my mothers, Susan, Susan, and Marguerite, I will call you right before I click submit, so thank you for being constant emotional supports to this work.

In loving memory of Ginger Simms – thank you for teaching me to unapologetically blaze my own trails and define my own happy.

Chapter 1: Introduction

Forest canopies influence local or microclimate conditions, which in turn alter ecosystem processes, including species interactions, disturbance dynamics, and successional trajectories post-disturbance (Costafreda-Aumedes et al., 2018; North et al., 2019; Zellweger et al., 2020). In the fire-disturbed forest of western North America, research supports that modern-day climate is not conducive for seeds of currently dominant forest species to establish (Davis et al., 2019b; Hansen and Turner, 2019). If microclimate conditions continue to surpass the growth thresholds for these seedlings, forest regeneration rates and future species composition will change (Stevens-Rumann et al., 2018). Given the globally increasing frequency and severity of fire (Westerling et al., 2006), we must accurately measure the microclimate conditions that influence ecosystem responses (De Frenne et al., 2021; Seidl et al., 2017). In fire disturbed environments, seedling success is mediated in part by the surrounding microclimate, dry and hot soils dramatically decrease successful seedling establishment (Hansen and Turner, 2019). However, there is a global lack of accurate microclimate models, particularly in these disturbed environments and given the compounding effects of a changing climate (De Frenne et al., 2021).

Developing accurate and spatially continuous models of microclimate temperatures and soil moisture – crucial variables of seedling success – is challenging because there is both a lack of field-based, in-situ forest climate measurements and a lack of accuracy in adjusting regional gridded climate models to microclimate scales (Lembrechts et al., 2019). In forests, temperature, soil moisture, and light availability vary dramatically at meter scales due to variations in microclimate drivers including forest structure, micro-topography, and other environmental factors (Chen et al., 2011). As discussed in more detail in Chapter 2, microclimate dynamics are driven by (1) topographic factors which modify the amount of available solar radiation, (2) soil composition, which determines both moisture retention and

thermal capacity, and (3) forest structure which intercepts solar radiation and can alter water budgeting (Oke, 2002). The accuracy of regional climate models, which have kilometer-scale resolutions, decreases in complex environments (Daly et al., 2008). These models fail to include high-resolution data and correction factors for forest canopies or topography (Lenoir et al., 2017). Models predicting future forest composition that rely on regional climate models may be inaccurate, because they rarely incorporate correction factors for forest structure and other microclimate drivers (Lenoir et al., 2017).

Forest canopies influence microclimate dynamics but quantifying the impact of a forest canopy is difficult because forest structures are complex. The presence of a forest canopy offers shade, alters near-surface airflow, and introduces energy interactions between trees and their abiotic environment (Geiger, 1950). Plant responses to globally warming temperatures are slower beneath forest canopies because canopies buffer warming regional climates (Zellweger et al., 2020). Further, forest canopies influence fine-scale moisture dynamics by blocking solar radiation and actively transpiring (Davis et al., 2019b). Forest canopies have a critical role in adjusting regional climate, and as a result, microclimate is impacted by canopy-altering disturbances, like fire, insect infestation, or windthrow (Dietz et al., 2020).

We generally assume forests offer a buffering capacity, sheltering near-ground or tree seedling environments from extreme temperatures (De Frenne et al., 2019). We cannot expect the same buffering in disturbed forests because the tree canopy is dramatically altered. A recent review of gaps in microclimate research by De Frenne et al. (2021) notes an overall lack of knowledge on how microclimates are buffered, offset, or potentially decoupled from open-air environments within "altered" forests landscapes. These altered landscapes include forested ecosystems subject to anthropogenic or natural disturbances (De Frenne et al., 2021).

Across disturbed and non-disturbed environments, we lack open-access gridded forest microclimate datasets necessary for predictive species distribution modeling (De Frenne et al., 2021). To

create these gridded microclimate datasets, we must develop methods to incorporate forest structure measurements in microclimate models (De Frenne et al., 2021). Historically, measuring forest structure at the meter-scale resolutions necessary for microclimate modeling was challenging (Maltamo et al., 2014). Forest structure data relied on costly and time-consuming field campaigns (Maltamo et al., 2014). New remote sensing techniques, like remotely piloted aircraft (RPAs), allow for spatially detailed and precise forest canopy structure measurements at spatial resolutions that align with microclimate dynamics (Goodbody et al., 2019; Zellweger et al., 2019). Specialized software can spatially overlap imagery collected from RPAs to create 3D models of forests (Colomina and Molina, 2014; Graham et al., 2019). RPA produced 3D models are particularly well-suited for modeling canopy height (Goodbody et al., 2019). However, their use to accurately estimate canopy cover or stand density is less established (Dietmaier et al., 2019). Research connecting remotely-sensed metrics of forest structure to microclimates is imperative for developing a practical standardized methodology for downscaling gridded climate datasets to near-ground environments (De Frenne et al., 2021).

Previously, measuring microclimate across a wide variety of altered landscapes was cost-prohibitive because of the high costs associated with microclimate recording equipment, including thermistors and moisture sensors (Lembrechts et al., 2021a). However, new inexpensive microclimate dataloggers that measure temperature and soil moisture allow for easy and comprehensive forest floor climate measurements (Wild et al., 2019). As a result, global datasets on key microclimate variables like soil temperature are increasingly available, although data are generally concentrated in the northern hemisphere, mainly Europe (Lembrechts et al., 2021b, 2021a). However, these global microclimate datasets can validate mechanistic (Maclean, 2020) or downscaled microclimate models (Dingman et al., 2013). Microclimate models are built from known relationships between microclimate and microclimate drivers like topography, soil composition, and forest structure. I argue that the current knowledge on the

impact and interaction of microclimate drivers is insufficient for modeling microclimate dynamics given increasing disturbance and climate change (De Frenne et al., 2021). To address this need for more research, my study leverages new remote sensing and sensor technology to investigate the relationship between a burned tree canopy and microclimate dynamics in interior British Columbia, Canada.

1.1 Research objectives

To increase our understanding of the tree canopy's role moderating the mean and range of microclimate values, I investigated the following research question: In a heterogenous post-disturbance landscape, what is the relationship between tree canopy and microclimate?

To answer this question, I posed two sub-questions:

Microclimate models lack standardized methodology for incorporating the impact of microclimate drivers (De Frenne et al., 2021). Importantly, we lack knowledge of the necessary spatial resolution to measure microclimate drivers (Maclean et al., 2021). In response to this research gap, I first asked what scale of spatial buffer to summarize canopy height data produces the strongest correlation between mean growing season microclimate and canopy height? After determining the best scale of spatial buffer to incorporate canopy in microclimate modeling, my second question was: What is the impact of differences in canopy height on the mean and range of microclimate variables known to influence forest regeneration? I assess this question at both growing season and monthly timesteps, which are timesteps known to influence tree seedling regeneration.

To answer these questions and provide relevant background, this thesis starts with a literature review, which includes a discussion of microclimate literature that emphasizes the importance of a forest canopy in microclimate dynamics and the value of novel remote sensing for microclimate modeling. The literature review is followed by a field-based study of post-burn forests that models how remaining forest structure, specifically canopy height, impacts microclimate dynamics. This thesis is focused on the

impact of a forest tree canopy on microclimate dynamics. The impact of understory vegetation is discussed in the literature review but was not the focus of this study. In the analysis chapter, in-situ measurements of soil moisture, near-surface, surface, and soil temperatures are modeled in relation to RPA-acquired canopy height and previously collected LiDAR topography data. The final chapter discusses the research outcomes, including the significance, limitations, and future work.

Chapter 2: Literature review of variables known to influence microclimate

Elements known to influence microclimate – henceforth microclimate drivers– include the surrounding topography, soil composition, understory structure, and tree canopy (Oke, 2002). This literature review begins by discussing each driver, followed by a review of our new approaches to measure these drivers with emerging technologies like RPAs (Fuka et al., 2016). Research gaps identified from this review include a need for microclimate research comparing the accuracy of high and medium-resolution spatial data in microclimate modeling (Table 2.1) and studies in naturally disturbed forests with minimal elevation changes (Table 2.2).

2.1 Major microclimate drivers

2.1.1 Topography

Topography influences the amount of solar radiation received at a surface, which governs heat exchange dynamics and impacts local temperature and soil moisture regimes (Oke, 2002). Site-level inclination, orientation, location, and elevation affect total surface solar radiation (Oke, 2002). Variation in site-level topography characteristics can produce temperature differences as high as 6 °C over several meters (Chen et al., 2011).

Topographic characteristics like aspect, slope, and terrain complexity impact temperature and moisture because these characteristics alter solar radiation and heat flow (Oke, 2002). In northern latitudes, a southwest-facing aspect on a moderate slope will have approximately 20% more solar radiation than a flat slope (Geiger, 2017). A 20% difference in solar radiation would produce temperature differences of about 6 °C over the day (Oke, 2002). Topography can also alter the water flow rate through a system (Dingman, 2015).

Site-specific soil moisture depends mainly on the flow rate of water through the system and the time since the last rainfall (Dingman, 2015; Halama et al., 2018). Water flow rates through a system are

influenced by soil porosity, soil depth, and previous precipitation, but soil moisture estimates improve when they consider surrounding topography (Fuka et al., 2016). Figure 2.1 illustrates the role of topography in moderating water flow rate, thereby impacting soil moisture. Rates of water flow are divided into three distinct zones, including the surface and below-ground unsaturated and saturated zones. Following a rain event, water moves from the surface to the unsaturated zone via a process called infiltration. Water continues to move into the saturated zone via a process called percolation (Dingman, 2015). Below-surface flow, including infiltration, percolation, and horizontal flow, is determined principally by the grain size of soil but is also impacted by the source area and subsurface topography (Dingman, 2015; Fuka et al., 2016). Surface topography affects the rate of overland flow (Dingman, 2015). Figure 2.1 does not discuss the impact of aspect and topographic complexity on evaporation and water flow, which can increase evaporation rates because they alter radiative heating and soil temperature (Halama et al., 2018).

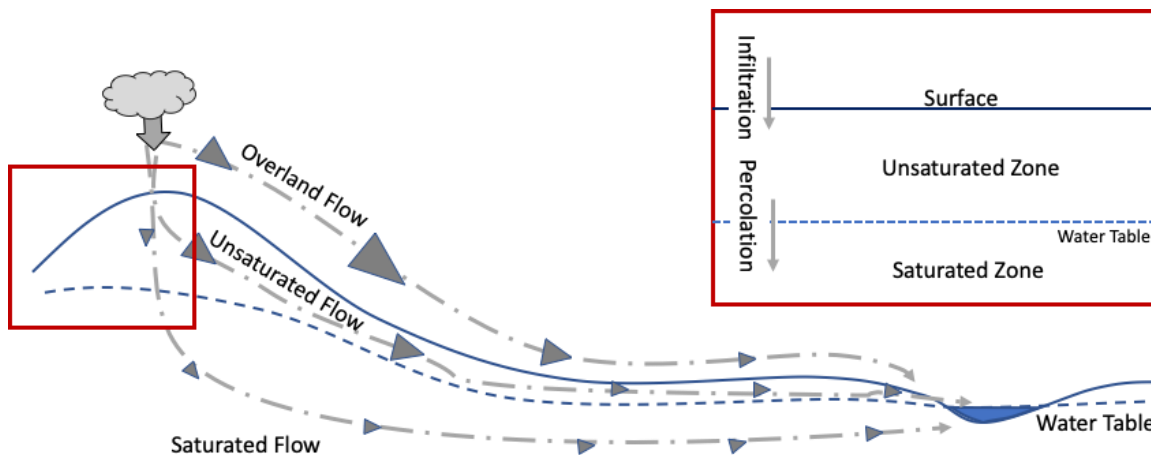


Figure 2.1 Schematic water flow rates in a system at different slopes with consistent soil composition. System water flow rates determine site-level soil moisture. Lateral flows are shown in the red-box subset. The size of the arrows on horizontal flows denotes relative flow rates. Note: There is no consideration of evapotranspiration.

Need for fine-scale topography in microclimate datasets – Topographic metrics are essential to include when downscaling climate models. Downscaling is a method used to predict gridded climate

datasets at higher spatial resolutions (Ashcroft and Gollan, 2012). Models of soil moisture and soil temperature are more accurate when they include high-resolution topography as a determinant of water flow and thermal heating (Fuka et al., 2016; Halama et al., 2018). Regional climate models generally explain climate at much larger kilometer scales; their accuracy decreases exponentially with finer spatial resolutions (Lembrechts et al., 2019). For example, PRISM (Parameter-elevation Regressions on Independent Slopes Model) model outputs are typically reported at 800 m²(Daly et al., 2008). When temperature estimates from PRISM are downscaled from 800 to 100 m², estimates capture only 20% of the observed temperature variance (Daly et al., 2008). PRISM uses topographic indices like location, elevation, coastal proximity, aspect, and surrounding topography to calculate the expected climate but relies on an elevation model with an 80-meter spatial resolution (Daly et al., 2008). Interpolated climate models, like PRISM, fail at these higher resolutions for two reasons (1) topographic variation, including aspect and elevation influence temperatures at resolutions finer than 80 m (Maclean, 2020), and (2) microclimate temperature dynamics are poorly explained by topographic indices alone (Jucker et al., 2018b).

2.1.2 Soil

Soil composition also influences microsite temperature, water availability and flow, and is thus an important variable to consider when modeling microclimate (von Arx et al., 2013). The thermal diffusivity – which is the rate that soil temperature changes with a temperature gradient and heat capacity – defined as total heat a soil can store, determines the rate and extent that heat from the surface transfers into the ground (Zhu et al., 2019). In dry periods, soil loses thermal regulating capacity because soil particles have a lower heat capacity than water molecules (Oke, 2002). Soil moisture content is controlled in part by soil particle size, which determines soil matric potential, the ability of soil particles to retain water via capillary action. A soil with a high matric potential, like clay or silt, generally has

lower temperatures and retains moisture for an extended period (Rodriguez-Iturbe et al., 1999). Soil moisture content is also heavily impacted by the depth of the soil itself. Deeper soils can accumulate more water during a rain event, so they also stay moist longer (Rodriguez-Iturbe et al., 1999). The water flow rate from the soil via evaporation or below-surface flow decreases logarithmically as the soil dries because of the adhesive properties of water (Dingman, 2015). Soil composition is then a determinant of hyperlocal temperature and moisture regimes because it influences heat and water flux in near-ground locations. However, preliminary research at field sites with relatively homogenous soil composition supports high-resolution topography better explains soil moisture dynamics than soil type (Kemppinen et al., 2018). Thus, acquiring high-resolution soil type data for microclimate modeling is likely a lower priority than high-resolution topography and forest structure data (Kemppinen et al., 2018).

2.1.3 Understory structure

Models of forest microclimate support that understory vegetation is a significant predictor of microclimate dynamics, particularly for maximum temperatures and vapor pressure deficit (Haughian and Burton, 2018; Kovács et al., 2017; Prévosto et al., 2020). At small scales, vertical differences in vegetation structure are the most important factor for altering energy budgets (Oke, 2002). Vegetation alters the energy budget by (1) preventing solar radiation from reaching the forest floor, (2) introducing vapor near the surface via transpiration, and (3) altering the formation of the boundary layer, which impacts both latent and sensible heat flux (Oke, 2002). Generally, the impact of vegetation on buffering capacity is greatest when the understory vegetation is tall or structurally complex (Prévosto et al., 2020), when overstory structure is minimal (Eskelson et al., 2011; Prévosto et al., 2020), or in summer months (von Arx et al., 2013). Studies have also shown that the impact of the understory vegetation is dependent on vegetation type (Haughian and Burton, 2018). A study of the microclimates in British Columbia found that lichen dominant forest plots were drier than plots with moss or other vegetation. They suggest

that lichen were both more likely to grow in dry environments and that their presence contributed to overall site dryness (Haughian and Burton, 2018). In disturbed forests, the influence of understory vegetation can be large because understory cover, height, and diversity generally dramatically increase post-disturbance while overstory structure decreases (Owen et al., 2020).

Understory vegetation plays a vital role in moderating microclimate environments, but quantifying the impact of vegetation is difficult because temporal and spatially continuous measurements of vegetation structure are hard to acquire (Blonder et al., 2018). Vegetation structure in disturbed environments is dynamic both seasonally and in the years after a disturbance (Andrade et al., 2021; Owen et al., 2020). While the role of understory vegetation dynamics on microclimate is clear (Prévosto et al., 2020), measuring and incorporating the impact of understory vegetation on microclimate is difficult (Blonder et al., 2018). Understory measurements made via remote sensing generally underperform compared to field-based measurements (Talucci et al., 2020).

2.1.4 Tree canopy

The ability of solar radiation to reach a near-ground location is a function of slope, aspect, and canopy interference (Geiger, 1950). Canopy interference can be defined as anything that prevents light from reaching the forest floor, including understory vegetation. However, the focus of this literature review section is on the impact of a tree canopy. Generally, decreasing tree cover increases solar radiation, which warms the soil and the air temperature of that area (Vanwalleghem and Meentemeyer, 2009; von Arx et al., 2013). The degree of warming is highly variable in different canopy conditions. Light infiltration ignoring the impact of topography is mainly determined by the leaf area index (LAI), a measurement of the photosynthetically active area. LAI is greatest in forests with high canopy cover, but LAI varies based on the stand age and type. Young and old forests have more light than mid-aged forests, which have higher tree densities and canopy cover (Geiger, 1950).

Site-level temperature changes with tree density and canopy cover, but the relationships vary across forest types (De Frenne et al., 2019). A study across a gradient of harvesting densities, which in turn reduced tree canopy cover, found that the site temperatures were not statistically different across the remaining tree densities (Chen et al., 1999). Conversely, a study of temperature in a selectively logged Bornean forest found canopy height and density were a strong driver of air temperature and vapor pressure deficit (Jucker et al., 2018b). Other studies have shown that the influence of tree canopy on microclimate is dependent on the type of forest (broadleaf vs. conifer) and season. In a study comparing broadleaf to pine tree canopies, temperatures beneath a pine canopy differed less from regional climate models compared to temperatures beneath broadleaf forests (von Arx et al., 2012). These differences are important to quantify because they determine the degree of warming experienced at a site, which is often but not universally buffered from the warming of the macroclimate (Zellweger et al., 2020).

Tree canopies can also influence soil moisture in three key ways: canopy (1) decreases the water a site receives, canopy interception, (2) withdraws water via the process of transpiration, and (3) increases the height and thickness of the boundary layer, which decreases latent heat flux (Dingman, 2015). Ecohydrological processes can then increase and decrease water flux, making the relationship between tree canopy and soil moisture harder to predict than temperature. Figure 2.2 shows a simple schematic of water flow with vegetation. Starting at the source, the total amount of precipitation an area receives decreases through canopy interception. Tree canopy interception can play a substantial role in total moisture input into the system. A study of post-burn forests in New Mexico found that areas with open tree canopies had seasonal snow depths 20 cm greater than those in unburned closed canopies (Harpold et al., 2014). Increasing tree canopy cover and density increase both interception and vegetation water demands via transpiration. Tree removal can increase soil moisture and ground-water percolation at the hyperlocal and catchment-wide scale (Beudert et al., 2015; Clark et al., 2014). As the

canopy influences the amount of solar radiation and winds that sites experience, the presence of a canopy can decrease the rate of evaporation from the soil surface (Oke, 2002). The degree of tree canopy interception is dependent on forest type, density, and total coverage immediately surrounding a site, resulting in highly site-specific soil moisture dynamics (Goeking and Tarboton, 2020; Rutter et al., 1971).

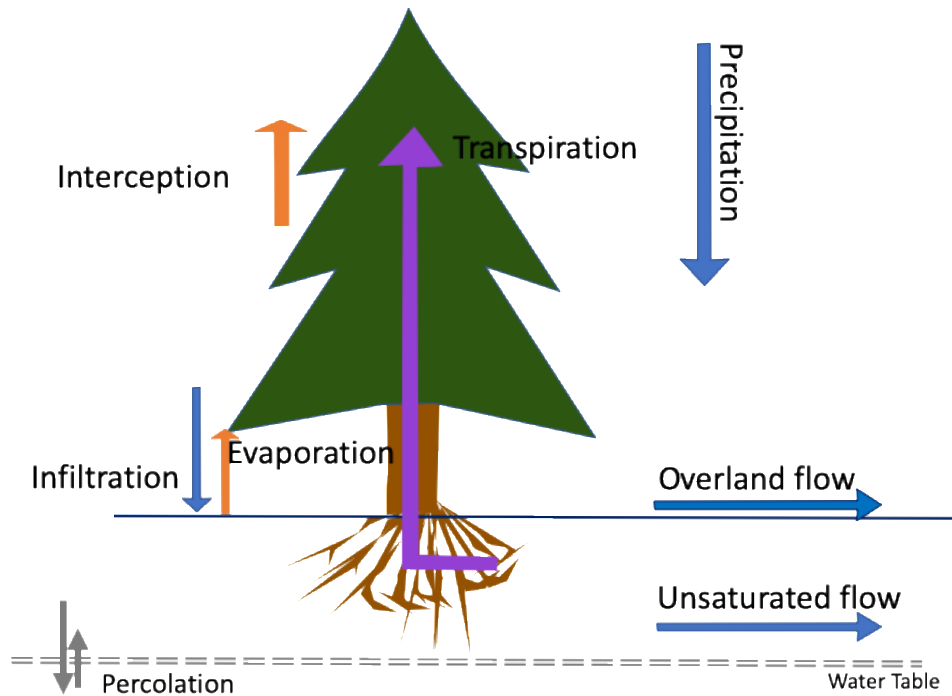


Figure 2.2 Schematic of water flow on a vegetated surface. Arrows show the approximate scale of relationships.

2.2 Differences in microclimate dynamics following tree canopy disturbance

There is strong support for tree canopy buffering of temperatures, protecting surface environments from climate change (Zellweger et al., 2020). However, the inclusion of tree canopy information in microclimate models is lacking: in a review of studies to enhance microclimate modeling, only half of the studies incorporate any metric of forest biota (Lenoir et al., 2017). Further, research suggests that the deviance between open-air environments and forested environments may be greater with higher average temperatures (i.e. climate change enhances the importance of a tree canopy) (Thom

et al., 2017). In this case, forested environments do not only buffer from regional climates, they completely decouple with their own unique climate dynamics (De Frenne et al., 2021). The theorized increased influence of a tree canopy with climate change raises important questions on how microclimate dynamics observed in disturbed forest canopies may change in combination with a changing climate (De Frenne et al., 2021). Table 2.1 outlines research studies on tree canopy impacts of microclimate in disturbed environments. These studies support that decreases in tree canopy – like canopy height, cover, and basal area, increase near-surface temperatures. However, this relationship varies from linear (Heithecker and Halpern, 2007) to non-linear (Jucker et al., 2018b; von Haden et al., 2019). Similarly, the relationship between soil moisture and forest structure may not be significant (Heithecker and Halpern, 2007) or may be negatively correlated (Ma et al., 2010). Decreases in a forest canopy associated with disturbance also increase the influence of topography (Kermavnar et al., 2020) or edge effects (Latimer and Zuckerberg, 2017) on temperature and humidity dynamics. Notably, relatively few studies investigate the role of a natural disturbance on microclimate dynamics (Table 2.1). Natural disturbances may present different successional trajectories because they produce extremely heterogenous overstory structures (Breshears et al., 1997; Thom et al., 2017).

In a high severity fire, where tree canopy cover decreases, the impact of the remaining overstory structure on temperature and moisture dynamics is not well defined. A detailed review of the effect of tree canopy disturbance, like fire or bark beetles, on soil moisture, found that of the 18 papers included in the review, approximately equal numbers found soil moisture (1) did not change, (2) decreased, or (3) increased after removal of the tree canopy (Goeking and Tarboton, 2020). These results suggest that differences across sites and ecosystems produce different moisture regimes after a forest disturbance. While this seems obvious, variable soil moisture responses could be explained by spatial and temporal differences in post-disturbance under and overstory structure, including canopy height and closure

(Andrade et al., 2021). Research on the interaction of canopy and microclimate is necessary as many papers on microclimate dynamics do not include measures of moisture or humidity (De Frenne et al., 2021; Lenoir et al., 2017). In a review of microclimate research to inform climate modeling, three of 14 papers included measurements of moisture (Lenoir et al., 2017). In my own review of the impact of canopy disturbance on microclimate, four of ten papers include some measure of moisture (Table 2.1).

In many studies modeling microclimate dynamics post-disturbance, overstory structures have less of an influence on microclimate than topographic characteristics (Dietz et al., 2020; Latimer and Zuckerberg, 2017; Ma et al., 2010). However, most of the studies in my review crossed large elevation gradients (Dietz et al., 2020; Heithecker and Halpern, 2007) and few focused on particular study sites (Anderson et al., 2007; Kermavnar et al., 2020; Ma et al., 2010). Studies that focus on microclimate dynamics at one field site find that elevation plays a minor role in microclimate (Kermavnar et al., 2020) or that elevation has the largest impact on observed microclimate (Ma et al., 2010). Thus, research in areas that limit the influence of other microclimate drivers, like elevation and aspect, is needed to clarify the impact of overstory forest structure on microclimate (De Frenne et al., 2021). There is also an additional gap in the literature on the impact of disturbed forest overstory on microclimate moisture dynamics (Table 2.1, Lenoir et al., 2017). Shifts in microclimate dynamics that occur in tandem with disturbance changes in the overstory and climate change threaten western North American forest resiliency and ecosystem services by impacting seed establishment (Hansen and Turner, 2019; McDowell et al., 2020)

Table 2.1 Selection of microclimate studies in disturbed forests. Studies quantify the impact of an overstory (canopy height, density, cover) gradient on microclimate dynamics. Studies that consider natural disturbances are colored in grey.

Study	Forest Type	Disturbance Type	Overstory Metric	Temperature	Soil Moisture or VPD	Findings
Kermavnar et al. (2020)	Fir-beech forest	Harvest	Canopy density	X		With decreased canopy density temperatures and temperature ranges increased, Relative humidity decreased, Vapor pressure deficit increased
Dietz et al. (2020)	Temperate forest	Windthrow	Canopy closure	X		Temperatures not significantly impacted by gap size Temperatures in forest gaps not different to areas with high canopy closure Elevation was the strongest driver of temperature differences
Davis et al. (2019)	Coniferous forest (across a climate gradient)	Large canopy gaps (disturbance type variable)	Canopy cover	X	X	Maximum growing season temperature decreased with increasing canopy cover (buffering capacity increased). This effect was most substantial in forests with high rates of ET. Maximum VPD decreased with increasing canopy cover; effect most substantial in forests with high ET rates
Jucker et al. (2018)	Tropical old-growth dry forests to oil palm plantations	Harvest	Canopy height and LAI	X	X	Canopy (height and leaf area index) explained 40% and 21% of the variation in maximum temperature and mean temperature, respectively Vapor pressure deficit, mean and maximum temperature decrease nonlinearly with canopy height. Effects are minimal when measured canopy surpasses 20 m.
<u>Greiser et al. (2018)</u>	Boreal coniferous forest	Harvest	Basal area and canopy cover	X		Impact of forest structure on temperature varies seasonally, canopy has the largest impact peak summer. Elevation determines fall season dynamics, but plays a smaller role in the rest of the year

Study	Forest Type	Disturbance Type	Overstory Metric	Temperature	Soil Moisture or VPD	Findings
Latimer and Zuckerberg (2017)	Temperate forest	Harvest and agriculture	Tree density and basal area	X		Tree density was a strong descriptor of winter maximum temperature, but elevation was the best descriptor of mean and minimum winter temperatures There was an interaction between the tree density and edge-effects, where lower tree densities had greater edge effects.
<u>Frey et al. (2016)</u>	Conifer forest	Harvest (studied a forest-mosaic)	Forest structural Complexity	X		Combined the impact of forest vegetation variables in modeling (study cannot delineate between overstory and understory impact) Impact of forest structure on microclimate varies seasonally Elevation had the most impact on temperature Forest structural complexity influenced temperature variability More complex and thereby were cooler
Ma et al. (2010)	Mixed conifer	Cross of harvest and fire	Canopy cover and basal area	X	X	Elevation had the most impact on temperatures High canopy cover influenced soil temperature and moisture, where soil temperatures were lower, and moisture was greater
Anderson et al. (2007)	Conifer forest	Harvest	Basal area and canopy cover	X		Large patches increased air temperatures by approximately 3 °C Thinning had a less extreme impact on temperature compared to patch dynamics
Heithecker and Halpern (2007)	Conifer forest	Harvest	Canopy cover	X	X	Temperatures decreased linearly with increasing canopy cover Soil moisture shows no apparent relationship to changing canopy

Motivations for improving post-disturbance microclimate modeling – To briefly underscore the importance of accurate modeling of post-disturbance microclimate conditions, many components of forest succession are influenced by microclimate dynamics. Microclimate impacts understory vegetation structure (Haughian and Burton, 2018), distributions of various vertebrate species (Varner and Dearing, 2014), and of particular importance to forest managers – seedling establishment (Hoecker et al., 2020). Successful seedling establishment is strongly impacted by proximal climate conditions, including light, water availability, and temperature thresholds (North et al., 2019). Most sub-alpine tree species have relatively small seeds with a large number of stock reserves (Lazarus et al., 2018). After germination, and once initial seed stocks are utilized, there is a heavy reliance on microclimate conditions for survival. Early growth stages without rootstock and ample water are at high risk of losing turgor pressure in the xylem, causing the seedling to "dry out" (Lazarus et al., 2018). As a result, relatively small changes in minimum soil moisture (~ 2 % - Kermavnar et al., 2020) or growing season surface temperatures (2 °C - Hansen and Turner, 2019) can have large implications on successful seedling establishment. Incorporating small-scale variation of forest structure and microtopography that ultimately determine microclimate is important for planting forests that successfully regenerate and are resilient to future disturbance (North et al., 2019).

2.3 The use of remote sensing to enhance microclimate understanding

New remote sensing technology offers the ability to map forest canopies at the high spatial resolution necessary for measuring major microclimate drivers, particularly after a disturbance (Goodbody et al., 2019). Historically, our ability to measure topography and canopy at sub-meter scales was limited. Developments in remote sensing in the 1990s, namely the integration of global positioning technology (GPS) with inertial measurement units (IMU) in aircraft, increased accuracy of aerial-based remote sensing from multi-meter resolution to sub-

meter resolution (Maltamo et al., 2014). A review of the application of remote sensing to microclimate modeling argues these remote sensing developments allow for more spatially complete and accurate models of microclimate in many different locations (Zellweger et al., 2019).

Generally, studies of microclimate dynamics support improved model fit when higher resolution data is included (Table 2.2). However, my review of the literature did not find a paper that compared the accuracy between high-resolution and medium-resolution spatial data for explaining microclimate dynamics (Table 2.2). Instead, most compare in-situ measurements to regional climate models (Table 2.2). Further, few studies look at the importance of spatial resolution for soil moisture dynamics. Research exploring the spatial resolution necessary for microclimate modeling is essential in light of the predictive study by Maclean (2019), which found that measurement accuracy increased at the 100 m resolution compared to the 1-meter resolution. Defining the relevant scale of spatial buffer to measure and incorporate the impact of forest structure and microtopography on site microclimate remains an open and necessary research area for producing gridded microclimate maps (De Frenne et al., 2021).

Table 2.2 Studies comparing spatial resolution used to build either predictive or explanatory microclimate models. Studies limited to those that either downscaled regional climate models or compared regional climate models to in-situ measurements.

Study	Microclimate Variables Measured	Spatial Resolutions Considered	Findings
Maclean (2020)	Free-air temperature, soil moisture	1 m, 100 m	Temperature data had a lower error at 100 m. Soil moisture data were not compared.
Lembrechts et al. (2019)	Free-air temperature, Surface Temperature, Soil Temperature	30" to 1" (arc-seconds) compared to in-situ measurements	In-situ data improved overall model fit, compared to 30m resolution data. This trend was strongest, particularly for wintertime soil temperatures.
Lenoir et al. (2017)	Free-air temperature	25 m and 50 cm	50 cm data improved accuracy of free-air temperature monitoring
Ashcroft et al. (2012)	Free-air temperature	1, 5, 25 km compared to in-situ measurements	1 km grid produced the slightest offset from temperature measurements
<u>Dingman et al. (2013)</u>	Free-air temperature	30 m and 2m downscaled with lapse-rate equations compared to in-situ	Accuracy improved with 2m downscaling, particularly for maximum temperatures and less for minimum temperatures

2.3.1 Remotely piloted aircraft for high-resolution measurements of forest structure

Novel technologies like remotely piloted aircraft (RPAs) are helpful because they can compare between high (meter) to medium (tens of meters) spatial resolution forest-canopy measurements as they measure forest structure at high resolution with lower costs than conventional piloted aircraft (Goodbody et al., 2019). RPA-measured metrics have been well correlated to vegetation metrics for both silvicultural purposes and general land assessment (Tompalski et al., 2019). In areas where canopy cover is open, RPAs have been used to create highly detailed maps of burn severity or seedling presence (Arkin et al., 2019; Feduck et al.,

2018) and RPAs have been used to model canopy height over forest stands in topographically diverse areas (Salamí et al., 2014).

High spatial resolution aerial imagery from RPAs can be used to create 3D models of surface structure. By spatially overlapping aerial photos, specialized software can identify common points. Angles between common points can then be collated via a process called digital aerial photogrammetry (DAP). Collated points and images are used to create point clouds and orthorectified images (Colomina and Molina, 2014; Graham et al., 2019). Studies demonstrate the capacity of RPA collected imagery to map canopy height, tree crown condition, and canopy density across a gradient of landscapes with high accuracy (Chisholm et al., 2013; Salamí et al., 2014; Tomaščík et al., 2017; Wallace et al., 2016). Orthorectified images and DAP-generated point clouds can be used to create a 3D model of structural and spectral elements for high accuracy remote sensing (Colomina and Molina, 2014).

DAP models can be used to create accurate and low-cost estimates of canopy height (Goodbody et al., 2019). However, because DAP relies on 3D structures captured from vertical imagery, the technology is limited for estimating specific forest structural metrics and topography. Forest structure metrics that give estimates of below-crown structure, like LAI are not well modeled with DAP (White et al., 2018). Fortunately, LAI is generally correlated to canopy height (Hardwick et al., 2015) – where RPA measurements are highly accurate (Wallace et al., 2016). However, the correlation of LAI and canopy height likely differs in disturbed environments because these environments have highly heterogeneous canopy structure and forest gaps (Tomaščík et al., 2017). The accuracy of DAP topography models, namely digital elevation models (DEMs), decreases in areas of high-canopy cover (Graham et al., 2019), so research often combines DAP with LiDAR-derived digital elevation models (DEMs) (Wallace et al., 2016). Light detection and ranging (LiDAR) uses a laser that can penetrate forest canopy to produce

high-resolution topography models (Frolking et al., 2009). The standard practice for creating canopy height models from DAP is to normalize DAP models to LiDAR-derived DEMs (Goodbody, 2019).

LiDAR data for topography is necessary for DAP modeling, but multiple acquisitions of LiDAR to gather current forest structure data can be cost-prohibitive (Wallace et al., 2016). LiDAR is particularly useful for remote sensing because it can characterize the forest structure and topography when spectral imagery cannot (Wallace et al., 2016). LiDAR metrics of canopy cover, density, and leaf area index have high accuracy (Dietmaier et al., 2019). However, the cost of LiDAR acquisitions forces researchers to balance cost-efficiency with increasing the spatial and temporal accuracy of forest structural models (de Almeida et al., 2020).

2.4 Conclusions from review

Microclimates are influenced by topography, soil, understory vegetation, and the presence of a tree canopy. However, research suggests that topography and overstory structure best explain microclimate dynamics, even when high-resolution soil data are available (Kemppinen et al., 2018). In disturbed environments, the relationship between a tree canopy and near-ground temperature and moisture is variable (Table 2.1). Further, a limited number of microclimate studies assess the importance of forest canopies on soil moisture dynamics (Table 2.1). Novel technology in remote sensing and microclimate measurements assists in a current rapid expansion of microclimate research (De Frenne et al., 2021). However, technology to measure understory vegetation remains an active area of research (Blonder et al., 2018; Talucci et al., 2020). Importantly, research that assesses the influence of the spatial resolution of canopy metrics, including high-resolution RPA data for accurate microclimate modeling, is lacking (Table 2.2).

Chapter 3: Canopy height effects on the growing season and monthly microclimate in a burned forest of British Columbia, Canada

3.1 Introduction

Forests play a large role in microclimate temperatures and moisture regimes. Forests buffer from regional temperature extremes, but the relative effect of a forest canopy varies from ecosystem to ecosystem (De Frenne et al., 2019). For example, conifer canopies in Europe have a lower buffering capacity than broadleaf forests – conifer forests are warmer in warm months and cooler in cool months than broadleaf forests (von Arx et al., 2012). Further, recent work suggests that disturbance events that impact the canopy also alter the relative impact of topography on microclimate (Kermavnar et al., 2020). In harvest-disturbed forests of Europe, as tree canopy density decreases, the influence of topography on temperature buffering increases (Kermavnar et al., 2020; Lenoir et al., 2017). Loss of forest canopies could increase the temperature differences among aspects, where southern aspects would be warmer (Geiger, 1950; Kermavnar et al., 2020).

The impact of a forest canopy on water availability, like site-level soil moisture, is not as straightforward as temperature (Goeking and Tarboton, 2020). In fire-disturbed forests of western North America, some studies suggest that canopy loss increases evapotranspiration and decreases soil moisture (Beudert et al., 2015; Biederman et al., 2017). Other studies have found that tree canopy removal reduces transpiration rates and increases soil moisture (Reed et al., 2018). Building our understanding of the impact of a canopy on soil moisture is a crucial component of modeling regenerative success, as values of annual minimum soil moisture, and particularly early-season soil moisture, influence regeneration (Davis et al., 2019a).

Advances in microclimate modeling are facilitated by the decreasing cost of small, compact, and robust dataloggers – able to acquire the in-situ microclimate data at a high spatial and temporal resolution to then align to high-quality 3D forest structure models (Lenoir et al., 2017; Wild et al., 2019). Specifically, relatively inexpensive and easily installed microclimate dataloggers can measure the soil, surface, and near-surface temperature and soil moisture at a high temporal frequency and measurement accuracy (Wild et al., 2019). Using this new technology, microclimate fluctuations at the meter or sub-meter scales can be directly related to differences in forest canopy metrics like gap-fraction (Kermavnar et al., 2020), LAI, and canopy height (Jucker et al., 2018b). Canopy height is a particularly useful forest metric, because it is well estimated with new and inexpensive remotely piloted aircraft (RPA) technology (Goodbody et al., 2019) and is generally correlated with other canopy metrics like LAI (Hardwick et al., 2015).

Until recently, investigations in microclimate were limited because the acquisition of high spatial resolution data of variables known to impact microclimates, or microclimate drivers, like topography (aspect, elevation, and terrain) and tree canopy (height and cover) was difficult (Zellweger et al., 2019). Many studies instead used coarsely downscaled climate data to define climate differences among sites while simultaneously acknowledging the known inaccuracies of downscaling (Talucci et al., 2019). Further, approaches for incorporating microclimate drivers in microclimate modeling are not consistent, particularly in disturbed landscapes (De Frenne et al., 2021). A review of the application of remote-sensing data to microclimate dynamics argues that meter-or sub-meter-scale metrics are necessary to model microclimate variability (Zellweger et al., 2019). Advancements in remote-sensing technology, including RPAs and light detection and ranging (LiDAR) systems, allow cost-efficient acquisition of such high-resolution data, able to quantify overstory structure, like canopy height, with high spatial resolution – in some cases, at a

centimeter resolution (Goodbody et al., 2019). Combining in-situ data with remote sensing, prior work has defined the relationship between increasing canopy height on decreasing seasonal near-surface temperature in Indonesia (Jucker et al., 2018b) or decreased diurnal temperature variation in managed European forests as canopy density increases (Kermavnar et al., 2020).

Here, I capitalized on RPA technology and inexpensive microclimate sensors to investigate how forest canopy height, measured by RPAs, influences post-disturbance microclimate in a recently burned sub-boreal forest. I first investigated the degree to which higher spatial resolution improves the fit of microclimate models by asking: (1) What scale of spatial buffer does canopy height best predict microclimate? Given prior research (Lenoir et al., 2017), I expected the strength of the relationship between canopy height and microclimate to increase as buffer size decreased. Once I established the most relevant spatial buffer to summarize tree canopy metrics for modeling, I asked: (2) How do fire-induced changes in tree canopy impact the mean and range of soil, surface, and near-surface temperatures and soil moisture at timesteps known to influence seedling establishment – (2a) the growing season and (2b) month-to-month. Over the growing season, I hypothesized that shorter canopies would lead to warmer and drier landscapes and increase the daily range in microclimate values. As coniferous forests do not have major seasonal changes in overstory structure, I assumed that the effect size of canopy height would remain constant across months of the growing season. As my field measurements cross a gradient of fire severity, our microclimate findings are discussed in the context of fire disturbance events. My results examine if we should expect burned forests to have differing microclimates from their non-burned counterparts (Davis et al., 2019b). My work additionally exposes an opportunity to model microclimate dynamics in a diversity of locales and in different environments by capitalizing on advancements in microclimate measurement and remote sensing technology.

3.2 Methods

3.2.1 Study area and forest plots

My study was located at the Alex Fraser Research Forest Gavin Lake Block (AFRF) 60 km north of Williams Lake, British Columbia, Canada (Figure 3.1). Elevation ranged from 600 – 1250 m. AFRF is located within the Prouton lakes fire boundary (C30870), which burned approximately 1000 ha of the 6000 ha AFRF forest in 2017. The AFRF field site on a south-facing slope, dominated by dry areas with shallow and coarse soils and some bedrock protrusions (Klinka et al., 2004). The study plots were in the sub-boreal spruce ecosystem zone where Douglas-fir (*Pseudotsuga menziesii* var. *glauca*) was the dominant overstory species, and sub-dominant species included hybrid spruce (*Picea glauca* x *engelmannii*), lodgepole pine (*Pinus contorta*), red cedar (*Thuja plicata*), and trembling aspen (*Populus tremuloides*; Klinka et al., 2004).

In 2020, I established 10 one-hectare forest plots along elevation and fire severity gradients to capture a range of canopy height and its impact on microclimate. I calculated forest plot level burn severity using summer 2017 Landsat derived normalized burn ratio (dNBR) acquired after the fire (Miller and Thode, 2007). Fire severity was variable throughout the AFRF field site, ranging from low-severity ground fire to high-severity canopy fire. Forest plots were numbered from 1 to 10, where 1 had the lowest plot average of fire severity, and 10 had the highest.

3.2.2 Datalogger locations and data compilation

Microclimate measurements – I measured microclimate from early May 2020 to mid-October 2020 (the AFRF growing season). A total of 90 microclimate dataloggers were deployed across the 10 forest plots, which resulted in 9 dataloggers per plot. Dataloggers were spaced approximately 30 meters from each other, but actual distances varied from 15 to 35 m to avoid

edge effects associated with cut blocks and difficulties deploying loggers in rocky forest soils (see locations in orange on Figure 3.1). All global positioning system (GPS) locations and elevations in this study, including datalogger locations, were recorded with a Leica GS 14 system (Leica Geosystems). At each datalogger, I collected soil cores using a push soil sample probe. The volume of soil samples was variable because of large clasts. I classified samples using standard soil classification of percent silt, clay, and sand (ASTM Committee D-18 on Soil and Rock, 2017).

I used high-accuracy and durable TOMST TMS-4 dataloggers to record temperature and soil moisture at 15-minute increments (Wild et al., 2019). These 30 cm dataloggers defined our later microclimate variables of interest, including three temperature sensors at -8 cm (soil), 0 cm (surface), and 15 cm (near-surface) relative to the ground surface. Thermistors had an accuracy of 0.5 °C between 0° and 70°C. Soil moisture was calculated over a 15 cm depth, where sensor accuracy was high (~ 0.1 %) but variable among soil types (Wild et al., 2019). I converted raw logger output to volumetric soil moisture (vol %) using calibration curves for each soil type from the manufacturer-provided "TMS3_Calibr User Soil Properties" software and soil type as classified from field samples (Wild et al., 2019).

Removing erroneous microclimate data – Some microclimate dataloggers were disturbed or dislodged throughout the study, likely by grazing wildlife. Microclimate data were checked for incorrect or inaccurate measurements using field notes and data visualization. Data issues when dataloggers were dislodged or occasionally malfunctioned generally resulted in very high or low soil moisture counts or rapid changes in soil moisture. I removed these points by calculating the 7-day rolling means of soil moisture standard deviation (see Figure S1 for an example). Large changes in standard deviation between two days suggested errors in the

measurements, which I confirmed with visual data assessment. All microclimate measurements determined to be erroneous were removed from further analysis: 56,000 (4.3%) of the 1,283,819 measurements were removed from later analyses (Figures S2 and S3).

Means and mean daily ranges of microclimate variables – To align with past research on the importance of mean growing season climate on regeneration (Hansen and Turner, 2019; Hoecker et al., 2020), I took a simple mean of the microclimate variable over the growing season (May – October). To expand on prior research of the impact of forest canopy on the daily range of microclimate variables (Kermavnar et al., 2020), I took the mean of the daily range (maximum-minimum) over the growing season (May – October). I also calculated monthly means of the variables of interest for months with complete data (May – September) to address the impact of canopy on early and late season microclimates, periods within the growing season that influence regeneration (Davis et al., 2019; Carlson et al., 2020)

3.2.3 LiDAR-derived aspect data

The AFRF field site was flown in 2009 with a moderate density LiDAR coverage (for more details see Coops et al., 2009). From this LiDAR data, I derived a 1 m digital elevation model (DEM). Aspect (°) was extracted from the 2009 LiDAR DEM using the terrain raster function (Hijmans et al., 2015). Aspect was extracted from a 10 m radius around dataloggers (Table 1), based on prior findings of the most accurate measure of site-level aspect (Laamrani et al., 2014; Luo et al., 2019). I converted aspect to a metric of potential relative radiation using the following formula (Pierce et al., 2005):

$$Aspect_c = -\cos(45 - A) \text{ Eq. (1)}$$

Where $Aspect_c$ is converted from aspect (A), the DEM extracted aspect in degrees (°). In this equation northeast facing slopes scale to -1 and southwest facing slopes scale to 1.

3.2.4 Remotely piloted aircraft data and canopy height modeling

RPA data – I flew four RPA flights between June 28th and July 4th, 2020 to cover all datalogger locations, using a DJI Phantom 4 RTK (real-time kinetic) RPA. I used DJI Pro GS RTK software (*DJI GS RTK App*, 2020) to plan flights that covered the study area and followed LiDAR DEM-derived elevations. Flight height depended on a field assessment of safe distance from treetops and ranged from 70 - 80 m above ground. Details of the RPA, camera, and flight planning are included in Table S1. In each flight area, I established and geolocated a minimum of 5 and a maximum of 12 ground control points.

3D Point clouds and terrain-corrected orthophotos for each flight area were created from image tie-points and RTK GPS locations recorded by the RPA via Digital Aerial Photogrammetry (DAP, Goodbody et al., 2019). DAP uses image overlap and knowledge of camera locations to align images and then model the geometric relationships of objects. Before image alignment, I removed poor quality images (< 0.7 in image quality as estimated by blur in images) or images with high root mean square error (RMSE) in GPS locations (RMSE > 2.0 m). I aligned images using the RTK GPS positions from the aircraft (RTK photo alignment, Table S2). I then loaded ground control points and marked their locations on images within Agisoft Metashape software (Agisoft, 2018), realigning images with these additional locations (Ground Control Point photo alignment, Table S2). I removed ground control points with an RMSE > 2.0 m. The final accuracy of alignment ranged from 0.001 to 0.21 m (Table S2). To produce point clouds, I set parameters for a "high" point density with "mild" depth filtering. For each flight area, I used point clouds to produce a final georectified orthophoto (Figure 3.1). Point cloud density of all flight areas was reduced to 3500 points/m² for enhanced processing speed.

Canopy height modeling—Before building any digital surface models from point clouds, I aligned DAP point clouds to LiDAR point clouds using iterative closest point alignment (ICP)

from CloudCompare 2.6.3 open-source software (*CloudCompare*, 2020). ICP LiDAR-DAP alignment ranged from 0.9 to 1.86 m (Table S2). We normalized the heights of DAP point clouds to the 2009 LiDAR DEM with the lidR lasnormalize function (Roussel et al., 2021). Normalized DAP point clouds were then processed to create canopy height models in raster format with a 0.1 m spatial resolution (Figure S4). I verified canopy heights with field measurements from fifteen 6.5 m radius canopy verification plots randomly distributed in the study area (Figure 3.1, see Appendix C for a full description of the process and results). For microclimate modeling, I extracted the mean canopy height at five different radii (2, 5, 10, 15, 20) from the canopy height raster using the R raster extract function (Hijmans et al., 2015). Canopy height models were built using lidR (Roussel et al., 2020).

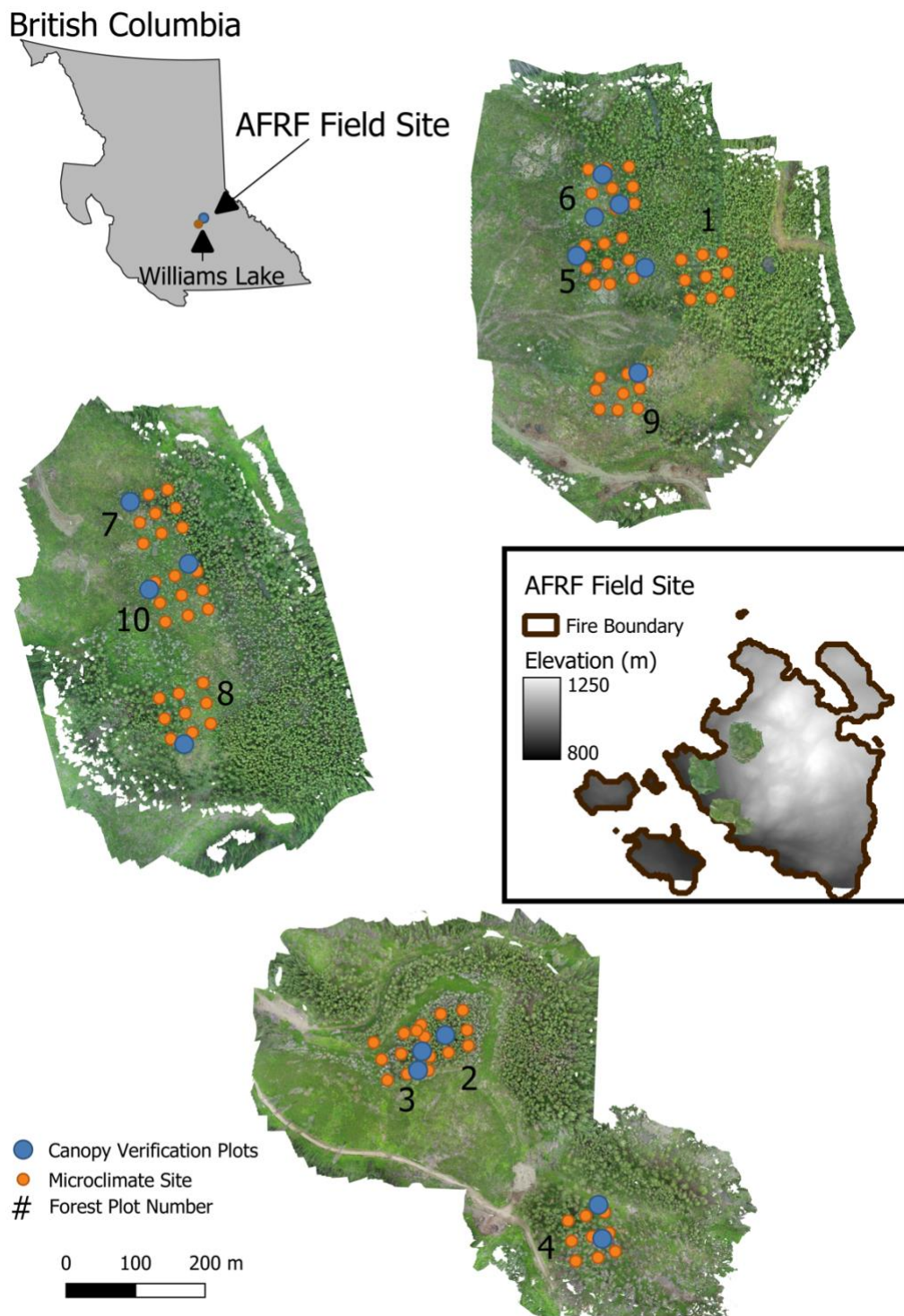


Figure 3.1 Orthophotos for four flight areas. Datalogger locations are noted in orange, and forest canopy verification plots in blue. Numbers correspond to forest plots. There are 9 dataloggers per forest plot. The inset map shows the 2009 LiDAR DEM and the 2017 fire boundary.

3.2.5 Analyses

3.2.5.1 Research question 1: Linear models to assess the scale of spatial buffer for canopy influence

To address the question of what scale of spatial buffer produces the strongest linear correlation between canopy height and the microclimate variables of interest, I fit simple linear models of the growing season mean microclimate variables as a function of canopy height, extracted at each canopy height radius (2, 5, 10, 15, or 20 m). I compared the coefficient of determination for each microclimate variable among the five radii. For each model, I checked assumptions of normality and equal variance using model residuals. Soil moisture models violated modeling assumptions, and thus I log-transformed soil moisture data. All subsequent analyses used the radius of canopy height that resulted in the highest model R^2 .

3.2.5.2 Research question 2: Mixed linear models to determine the impact of canopy height on microclimate variables of interest

Growing season means and mean daily ranges – I fit models to the growing season means and the mean daily ranges of the growing season for each microclimate variable of interest as a function of canopy height, elevation, and aspect (see Table 3.1). I included aspect and elevation in the models to control for their known influence on microclimate (Hoecker et al., 2020; Jucker et al., 2018a). I used the Pearson correlation coefficient to check for correlation in explanatory variables before building models. All Pearson correlation coefficients were below 0.50 (Table S3), an accepted thresholds for correlation in linear modeling (Dormann et al., 2013). I included forest plot as a random effect in the models to account for the lack of spatial independence among dataloggers within the same forest plot. I ensured all models met the linear model assumptions of normality and equal variance. For mean growing season soil moisture, and

mean daily range temperature models, values were log-transformed to achieve normally distributed errors. I first fit a full model:

$$v_{ij} = \beta_0 + \beta_1 \times DAP\ Canopy\ Height_{ij} + \beta_2 \times Elevation_{ij} + \beta_3 \times Aspect_{ij} + \gamma_j + \varepsilon_{ij} \mathbf{Eq. (2)}$$

where v_{ij} is the microclimate variable of interest (see Table 3.1 for list) at the datalogger i in plot j . β_{1-3} are the slope parameters associated with the explanatory variables, including canopy height for the radius with the highest correlation coefficient, LiDAR-derived aspect, and field-measured elevation. γ was random forest plot effect ($j = 1-10$ for each plot). I used likelihood ratio tests to identify optimal models.

Canopy height as a robust overstory structure metric – As microclimate dynamics are impacted by both canopy cover (Ashcroft and Gollan, 2012) and canopy height (Jucker et al., 2018b) I compared models built using DAP measurements of canopy cover and canopy height. Canopy cover and height were strongly correlated (spearman correlation > 0.8 for all radii of canopy height, Figure S8), and fitting models with canopy cover produced no differences in model effects nor parsimony. RPA measurements of canopy height are generally more accurate than canopy cover estimates (Dietmaier et al., 2019). Thus, I presented models built using canopy height data. However, based on the correlation between cover and height estimates, I argue canopy height was a robust metric of overstory structure for the field site’s fire-disturbed environment.

Monthly means – To understand how the relationships between canopy and microclimate may vary across months, I built separate models for each monthly mean of soil, surface, and near-surface temperature and soil moisture. To allow for comparison across models of different months, I fit the full model (Eq 2.) and did not reduce further. I compared the direction and

magnitude of the slope parameter estimate associated with canopy height in each month. When 95% confidence intervals of the estimated parameters do not overlap, I consider the parameters to be statistically different across months (Dai et al., 2021; Di Stefano, 2004; Scheiner and Gurevitch, 2001). I also reported the adjusted conditional R^2 (Nakagawa and Schielzeth, 2013) for mixed effects models calculated with the MuMin package (Barton and Barton, 2015) to show differences in models' goodness of fit month-to-month. I fit the mixed-linear models using the lme4 package (Bates et al., 2015). All processing was completed in R (R Core Team, 2019).

3.3 Results

3.3.1.1 Means (growing season and monthly) and mean daily ranges of microclimate variables

Growing season means and mean daily ranges – soil temperatures showed less daily variability and were, on average, cooler than surface and near-surface temperatures (Table 3.1). Surface temperatures were the warmest for the growing season, but soil temperatures had the highest maximum growing season temperatures (Table 3.1). Soil moisture had a high mean vol % content of 51 % and small-scale daily variability (0 - 1 vol %). There was a strong drying trend in soil over the course of the growing season (Figure 3.2 D).

Monthly means – Microclimate variables followed expected seasonal trends with peak temperatures in mid-summer and seasonal soil drying (Figure 3.2). Soil temperatures were cooler than near-surface and surface temperatures early in the growing season, which is also when soil moisture was high (Figure 3.2). Soil temperatures were the most variable across dataloggers, but variability decreased later in the growing season. Mean surface and near-surface temperatures were about the same in both July and August. Soils were driest in August, and soil moisture increased in both September and October (Figure 3.2).

Table 3.1 Summary statistics of growing season microclimate data and explanatory variables: canopy height, elevation, and aspect. Mean growing season values are the mean for the growing season. The mean growing season range is the mean of the daily range in microclimate variables. Aspect is presented in degrees, but models used a converted aspect (Eq 1).

		Minimum	Mean	Maximum	
<i>Microclimate variables of interest – Growing Season</i>	<i>Mean</i>	Soil (°C)	8.7	12.4	15.4
		Surface (°C)	9.7	12.8	15.1
		Near-Surface (°C)	10.0	12.6	15.0
		Soil Moisture (vol %)	30	50	80
	<i>Mean Daily Range</i>	Soil (°C)	1.2	3.19	7.56
		Surface (°C)	5.1	11.3	19.1
		Near-Surface (°C)	8.2	13.3	19.9
		Soil Moisture (vol %)	0	0	1
<i>Explanatory Variables</i>	DAP Canopy Height (m)	2.0	12.9	42.7	
	Elevation (m)	921	1029	1157	
	Aspect (degree)	38	219	314	

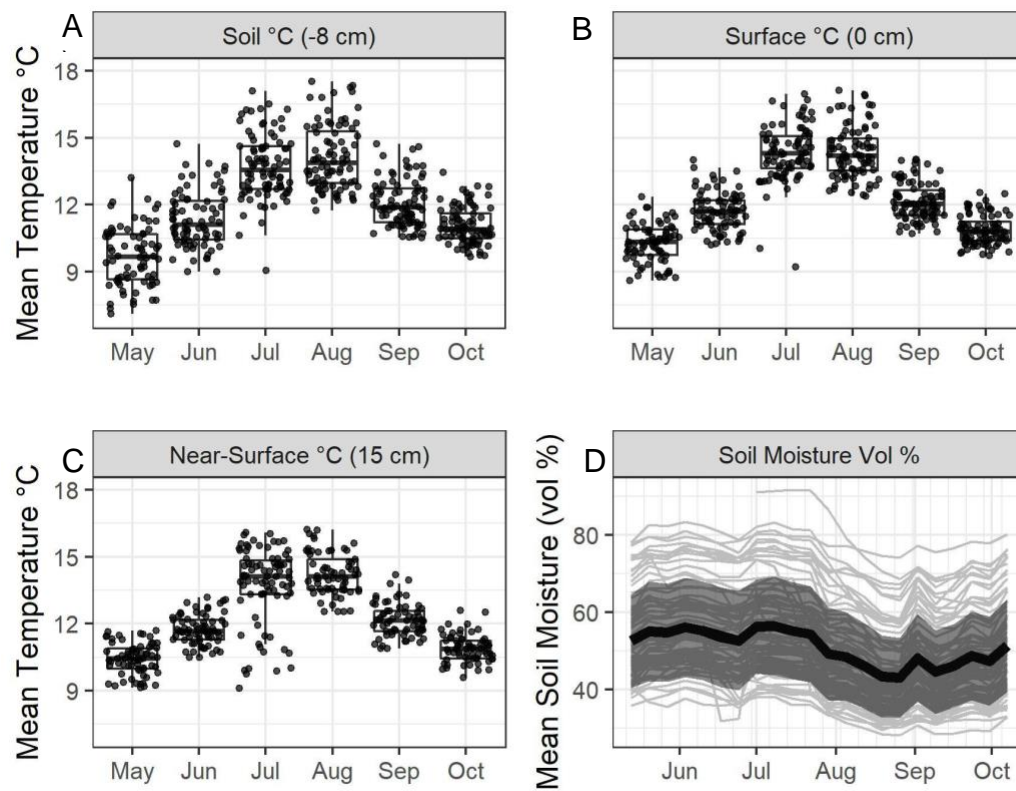


Figure 3.2 (A-C) Mean monthly temperatures and (D) weekly means of soil moisture for dataloggers. The dark line is the mean soil moisture for the AFRF field site, and the grey band is the standard deviation. Note: the high value in mean soil moisture is a datalogger in a wet location where equipment was removed early in the season. The equipment was replaced in July.

3.3.2 Research question (1): Linear correlation between canopy height and mean temperature and soil moisture differs as a function of spatial buffer

The coefficient of determination (R^2) between mean growing season temperature, soil moisture, and canopy height changed as a function of the spatial buffer used to summarize canopy height (Figure 3.3). As the area used to summarize canopy height increased, models explained more variability in mean growing season temperature, but less variability in mean growing season soil moisture. Canopy height summarized at 15 m best explained soil and near-surface temperatures and canopy height summarized at 20 m best explained surface temperatures. Differences in coefficient of variation between 15 and 20 m were small (difference between 15 and 20 m R^2 for surface temperature = 0.002); to stay consistent, all subsequent analyses of temperature used canopy height summarized by a 15 m radius.

The coefficient of variation between canopy height and mean growing season soil moisture was much lower than for mean growing season soil and surface temperatures (Figure 3.3, all $R^2 \leq 0.3$). The 2 m radius had the highest model R^2 between growing season soil moisture and canopy height – thus, I used a 2 m radius for all models of soil moisture ($R^2 = 0.07$).

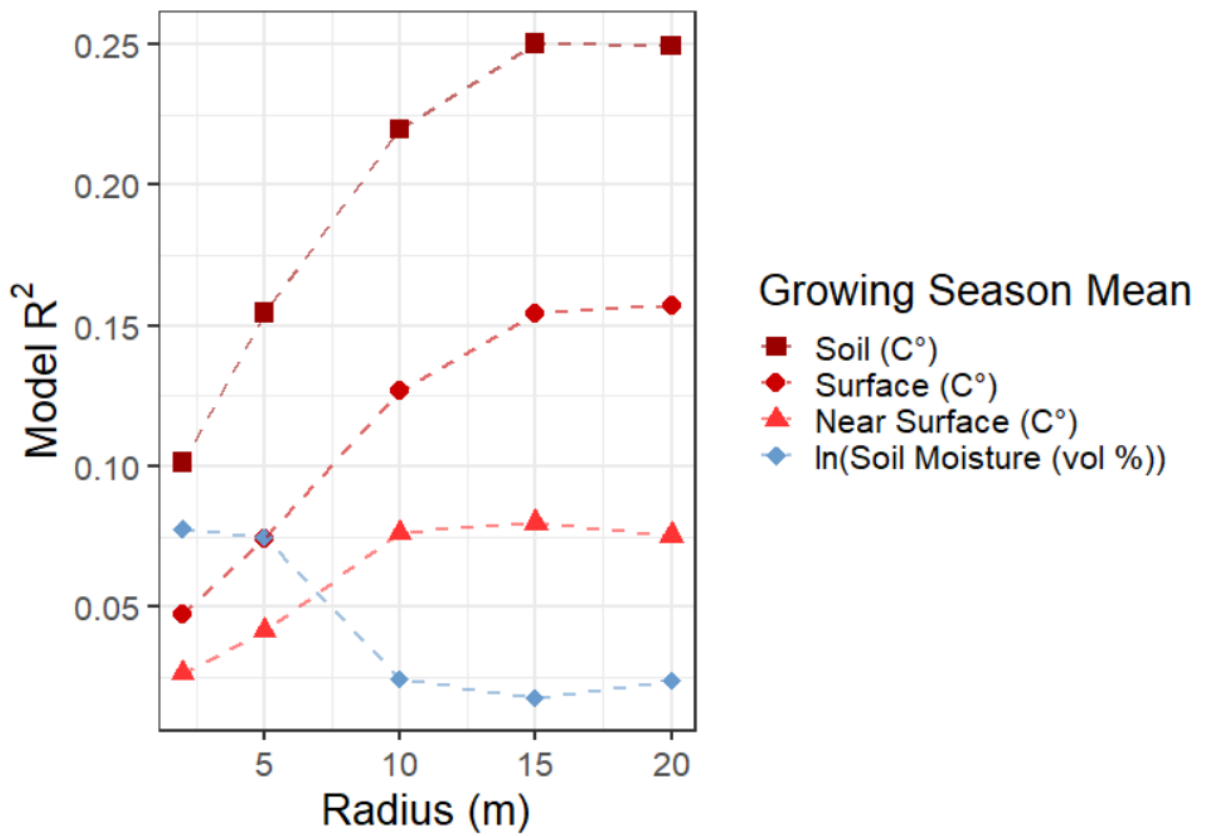


Figure 3.3 Model R² for microclimate growing season means with canopy height summarized with buffers of 2, 5, 10, 15, and 20 m radii. Points are colored by model type: soil – dark red, surface – red, near-surface – light red, Soil Moisture – blue. Note: these models do not include aspect and elevation included in later modeling

3.3.3 Question 2a: Canopy height consistently explains growing season microclimate

The best models for all growing season microclimate models (mean and daily range) include canopy height as an explanatory variable (Table 3.2). Mean growing season temperatures in the soil, at the surface, and near the surface decreased as a linear function of canopy height (Figure 3.4). Canopy height had the largest effect size in mean growing season soil temperature (Table 3.2). According to the model results, for every 10 m decrease in canopy height, mean growing season soil temperature increased 1.7 °C, compared to 1.4 ° and 0.9 °C for surface and near-surface temperatures, respectively.

There was an overall weak negative relationship between mean growing season soil moisture and canopy height, which was not as strong as the temperature relationships (Figure 3.4 and Table 3.2). In this study, a 10 m increase in canopy height was associated with a 9% decrease in mean growing season soil moisture. Some particularly tall canopies (> 15 m) had very low growing season soil moisture values (Figure 3.4). The two dataloggers with mean growing season soil temperatures less than ~10 °C were in wet locations (growing season soil moisture > 70 vol %) located in bogs or sphagnum moss.

Models of daily ranges showed similar trends to mean growing season models, where the mean daily range in temperature decreased with increasing canopy height. In these models, except for near-surface temperatures, including aspect and elevation as explanatory variables did not improve model fit and instead, canopy height alone produced the optimal model (Table 3.2). The near-surface temperature was the only variable for which aspect was significant – temperatures increased for southerly aspects (Table 3.2). Mean daily ranges of soil temperature, like the results of mean growing season models, were most influenced by canopy height differences (Figure 3.3). A difference of 10 m in canopy height was associated with a 1.5 °C change in the range of daily soil temperature. I observed daily oscillations in soil moisture across dataloggers (Table 3.1).

However, these daily ranges were not explained by full or reduced models using microclimate drivers (Table 3.2, Figure 3.4).

Table 3.2 Optimal models for mean growing season microclimate variables. The full model included canopy height, elevation, aspect, and plot as a random effect (Eq. 2). *Notes that the microclimate variable was log-transformed to meet model assumptions. Std. Dev is the standard deviation

		Canopy Height (m)		Elevation (m)		Aspect (converted)		Random plot effect (units match response variable)		Adjusted R ²	
	Model	β_1	Std. Dev	β_2	Std. Dev	β_3	Std. Dev	Range of γ	Std. Dev		
Mean	<i>Soil</i>	-0.202	0.029	-0.007	0.002			-0.163	0.319	0.150	0.42
	<i>Surface</i>	-0.133	0.024	-0.006	0.002			-0.176	0.423	0.193	0.38
	<i>Near-Surface</i>	-0.096	0.026	-0.005	0.002			-0.700	0.913	0.451	0.42
	<i>*Soil Moisture</i>	-0.009	0.003					-0.031	0.034	0.019	0.12
Daily Range	<i>*Soil</i>	-0.047	0.009					-0.052	0.035	0.029	0.27
	<i>*Surface</i>	-0.029	0.006					-0.090	0.078	0.062	0.35
	<i>*Near-Surface</i>	-0.020	0.005			0.009	0.023	-0.166	0.080	0.072	0.42
	<i>Soil Moisture</i>	0.000	0.000					-0.002	0.003	0.003	0.11

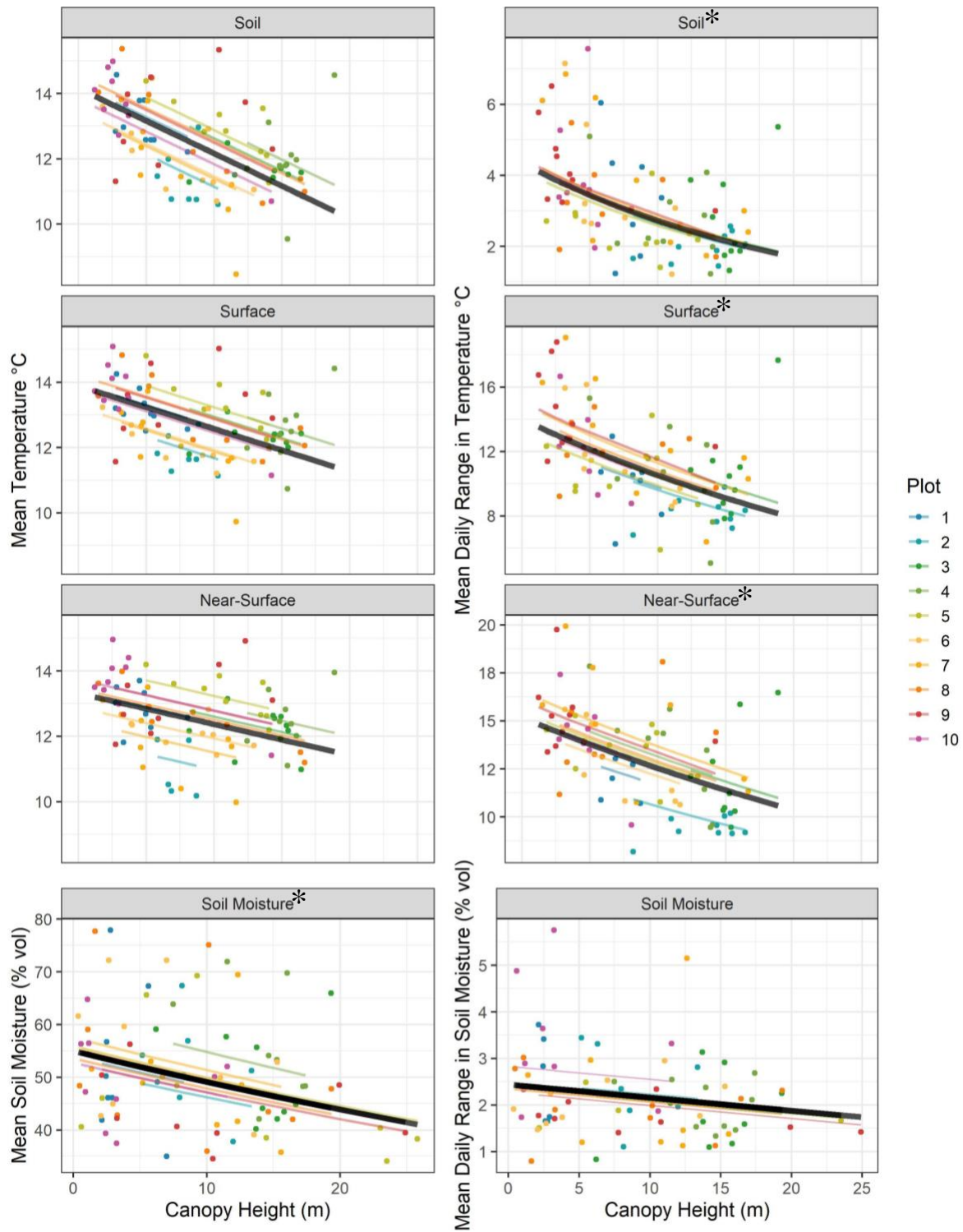


Figure 3.4 Mean growing season temperature and mean daily range as a function of canopy height.

Temperatures for soil, surface, and near-surface are shown in different panels. Points are colored by forest plot. Lines show predictions of mixed effects models. *Notes that the microclimate variable was log-transformed to meet model assumptions (including mean growing season soil moisture).

3.3.4 Question 2b: The impact of canopy height on monthly mean microclimate differs throughout the season

Models indicated differences in the relationship between canopy height and temperature response over the course of the growing season. Overall, explanatory power, based on the adjusted conditional R^2 of the monthly model (Eq 2, both fixed and random effects), was highest in the early growing season and decreased mid-summer (July, August - Figure 3.5e). The negative relationship between canopy height and mean monthly temperatures differed in magnitude across months and was greatest in July (Figure 3.5). However, the confidence interval for the effect size of canopy height was also greatest in this month (Figure 3.5 a - c). The impact of canopy height was weaker at the end of the growing season compared to the beginning (Figure 3.5).

Models of mean monthly soil moisture support canopy height did not influence soil moisture in the early season, but there was a negative correlation between canopy height and soil moisture in July, August, and September (Figure 3.5). The explanatory power of mean monthly soil moisture models was lower than temperature models; all adjusted R^2 for soil moisture were below 0.15, and adjusted R^2 was largest in the late summer (Figure 3.5).

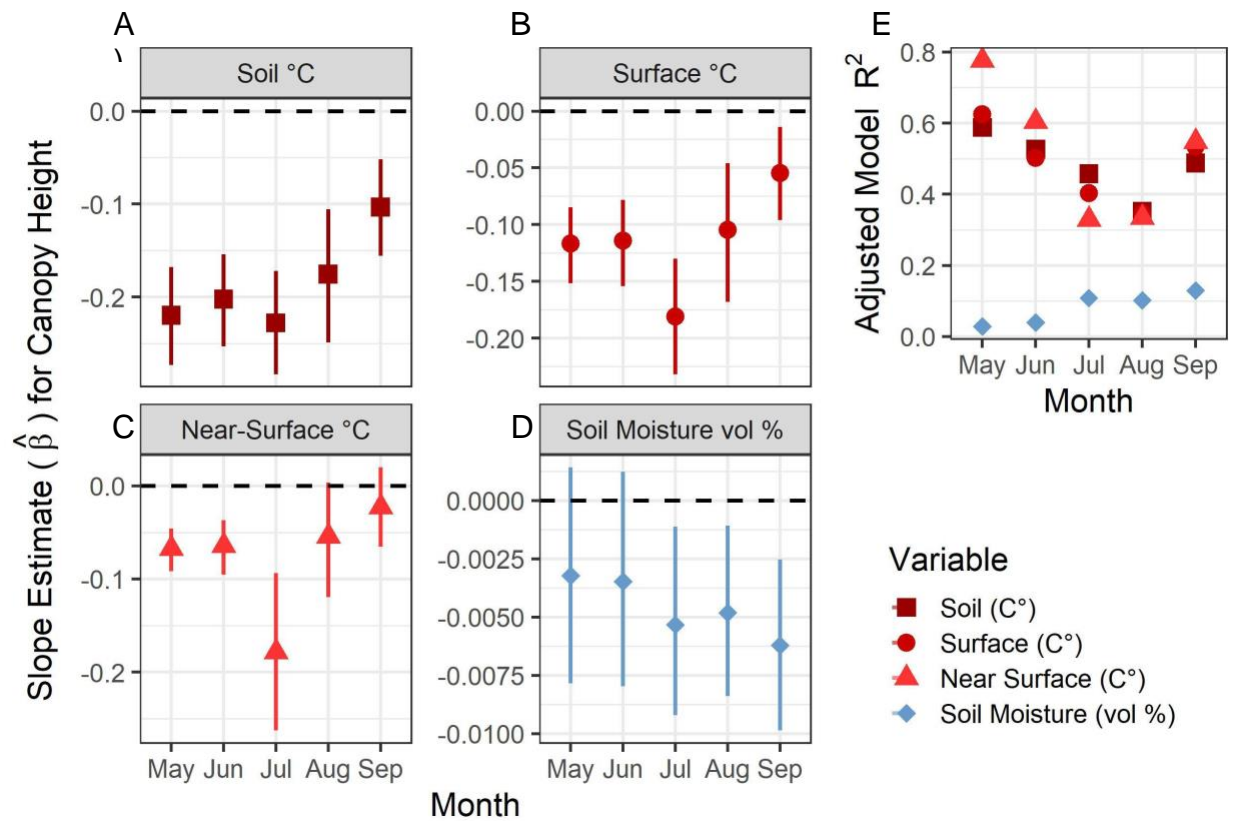


Figure 3.5 (A-D) Confidence interval and model estimate for canopy height to mean monthly microclimate variables (Near-Surface, Soil, Surface, and Soil Moisture). Points show model estimates for models fit to data by month. Bars are the 95% confidence intervals for the parameter estimate. Note: vertical scales differ by the panel. (E) Adjusted model R^2 for each monthly model. Color and shape align with microclimate variable.

3.4 Discussion

This study outlines a simple approach for remote-sensing-based microclimate modeling in fire-disturbed environments. Across a gradient of post-burn forest RPA based measurements of forest canopy height, which were strongly correlated to canopy cover, significantly explained temperature and soil moisture dynamics at the field site. Models explaining monthly microclimate and the importance of tree canopy have similar explanatory power to prior research studies using remote sensing (Greiser et al., 2018; Thom et al., 2020). Important for microclimate modelers – I found that the scale of spatial buffer necessary for microclimate modeling depends on the microclimate variable measured. Further, I found that the impact of

canopy height on temperature changed throughout the growing season. However, my high spatial resolution dataset poorly explained soil moisture, suggesting that control of soil moisture is influenced by variables difficult to capture with the remote sensing tools I utilized. Variables that could improve moisture modeling include understory vegetation, sub-surface topography, and litter dynamics, to name a few (Ma et al., 2010). In contrast to prior research, canopy height was more influential on mean growing season soil temperature than surface and near-surface temperatures (Ashcroft and Gollan, 2013). My study highlights the importance of including tree canopy in post-disturbance microclimate modeling – as differences in post-burn tree canopy were associated with microclimate differences known to impact regeneration (Hansen and Turner, 2019)

3.4.1 Tree canopy height explains microclimate temperatures over other known microclimate drivers

Canopy height significantly explained temperature over other known microclimate drivers like aspect and elevation. This finding is in contrast to past research where elevation is the most significant explanatory variable of microclimate temperatures (Dietz et al., 2020). However, the explanatory power of microclimate drivers is seasonally variable. The influence of elevation can be less in the growing season compared to winter (Greiser et al., 2018). Similarly, the impact of forest structure on microclimate is known to vary seasonally (Frey et al., 2016). Continuous microclimate measurements across seasons and years are needed to clarify the seasonally variable impacts of microclimate drivers like topography and tree canopy (Lembrechts et al., 2021a).

I observed that the effect size of tree canopy height was nearly double in magnitude in July, which is consistent with other studies that support canopy buffering is greatest mid-summer (Greiser et al., 2018; Kovács et al., 2017). A proposed hypothesis for mid-summer buffering is

that vegetation filters the same proportion, but an overall larger amount of solar radiation in high summer (Greiser et al., 2018). Ignoring the influence of topography and vegetation, summer insolation is greatest at these high latitudes (Geiger, 1950). Fire in boreal ecosystems is predicted to rapidly increase in frequency and area with global climate change (Hope et al., 2016). In response to this, I argue further research on mid-summer buffering within disturbed canopies at high latitudes is necessary as they may have unique microclimate dynamics due to strong summer insolation near the solstice.

Canopy height was more important for explaining soil temperatures than both near-surface and surface temperatures. Prior research has shown that near-surface temperatures are more sensitive to canopy cover than soil temperatures (Ashcroft and Gollan, 2013). Models built to improve soil temperature estimates should consider my study's differing results (Fuka et al., 2016; Lembrechts et al., 2020). The differing response between my findings and prior work could be due to the depth of soil temperature measurements. TMS-4 soil temperature sensors are at - 8 cm, where many soil temperature datasets are less than 5 cm below the surface (Ashcroft and Gollan, 2013; Lembrechts et al., 2019). In this case, the presence of a tree canopy may consistently moderate temperatures with increased depth. Soil temperatures near the surface could have different thermal dynamics due to increased soil organic content or exposure to near-surface air circulation (Oke, 2002). Expansion of research on the potential differences in the effect of tree canopy on soil temperature at different soil depths is essential for accurate microclimate modeling (Lembrechts et al., 2020).

Overall, my soil moisture findings add to the existing literature on the extensive variability in soil moisture response to a disturbed tree canopy (Goeking and Tarboton, 2020). I found a negative relationship between tree canopy height and soil moisture, but many studies in disturbed landscapes suggest there is a positive relationship (Goeking and Tarboton, 2020). This

finding underscores the importance of in-situ measurements, specifically in the context of disturbance in British Columbia (Talucci et al., 2019). In British Columbia, research suggests the soil moisture content is a better predictor of forest succession than regional climate conditions (Gendreau-Berthiaume et al., 2018). However, moisture conditions in fire-affected British Columbia forests are highly variable and poorly explained by the downscaled estimates of moisture (Talucci et al., 2019). I echo the calls of previous researchers for increased soil moisture monitoring in recently and non-recently disturbed forests across British Columbia (Haughian and Burton, 2018). These measurements will improve our capacity to build gridded microclimate maps accurate to the condition and type of forest (Maclean, 2020).

3.4.2 The impact of tree canopy on microclimate variables in the context of successful regeneration

The observed differences in soil and near-surface temperatures that correlated with canopy height have important implications for plant succession and regeneration success (Pincebourde and Salle, 2020). In particular, soil temperature, which I found to be the most impacted by changes in canopy height, is known to influence regeneration in the sub-alpine forests that encompass much of western North America's burned area (Hansen and Turner, 2019). In the context of my study, a 1.5 °C increase in soil temperature corresponded to a 10 m decrease in canopy height, which is approximately the mean difference in canopy heights of the high burn severity forest (10 and 9) and lower burn severity (1 and 2) plots. Prior to the fire, most forest plots had mean canopy heights within 4 m of each other, so I assume canopy height differences are predominantly a result of the fire. In Yellowstone's sub-alpine forests, as little as a 1 °C difference in growing season soil temperature resulted in a 60% decrease in *P. menziesii* (douglas-fir) and a 24% decrease in *P. contorta* (lodgepole pine) survival (Hansen and Turner, 2019)

I found that soils were drier under taller canopies, and this relationship was stronger in the late growing season. The overall change was small, but slight shifts in soil moisture ($> 2\%$ vol) can determine successful forest regeneration (Davis et al., 2019a). Successful regeneration is related to spring soil moisture and the driest conditions the site experiences (Lazarus et al., 2018). Sites beneath tall canopies with high canopy cover were drier in the late summer, suggesting that seedling regeneration under tall and less fire impacted forest canopies could be both moisture and light-limited (Legendre-Fixx et al., 2018).

Soil moisture in part moderates soil temperature as moisture content determines latent heat flux (Ashcroft and Gollan, 2013; Oke, 2002). Theoretically, locations with greater soil moisture should also be cooler because of the heat capacity of water (Geiger, 1950). However, my study found that drier and cooler locations were beneath tall canopies. This generally contradicts studies in other disturbed environments, where areas without forest canopies are generally both warmer and drier in the growing season (Braziunas et al., 2018; Davis et al., 2019a). However, my models generally poorly described soil moisture, supporting the need for continued in-situ measurements of soil moisture to clarify soil moisture characteristics in disturbed canopies (Goeking and Tarbonton, 2020; Zellweger et al. 2019).

3.4.3 Scale of spatial buffer necessary for microclimate modeling differs by microclimate variable, temperature, or soil moisture

My study found high resolution forest structure data predicted soil moisture better when summarized at finer scales. These results confirm the importance of the immediately surrounding tree canopy available solar radiation and ecohydrological dynamics (Oke, 2002). Results further suggest that soil moisture modeling requires metrics not easily measured with accessible and inexpensive remote-sensing technology. My findings are important given the overall lack of research connecting soil moisture dynamics to microclimate drivers at different spatial

resolutions (Lenoir et al., 2017). The overall lack of fit in soil moisture models confirms that soil moisture dynamics are complex, and the accessible and affordable remote sensing metrics I use in the present study do not capture important metrics like understory vegetation, litter, and sub-surface topography (Haughian and Burton, 2018; Kovács et al., 2017).

Contrary to prior research, my results suggest multi-meter spatial resolutions of tree canopy may better explain microclimate temperatures (Lenoir et al., 2017; Zellweger et al., 2019). Mechanistically, temperatures in a forest canopy may be better-modeled by metrics summarized at multi-meter scales because the temperature at microclimate level is controlled mainly by total incoming solar radiation, which is altered by leaf area index, a correlate of canopy height, complexity, and distance (Hardwick et al., 2015), slope and aspect (Geiger, 1950). Most studies on climate modeling accuracy use climate datasets interpolated to smaller scales and compare to in-situ measurements (Lembrechts et al., 2019; Talucci et al., 2019). My approach instead defines how the explanatory power of canopy changes as a function of increasing spatial buffer. Future research should capitalize on low-cost RPA measurements, and gridded climate estimates to clarify what spatial resolution of tree canopy efficiently improves microclimate modeling.

3.4.4 Improving microclimate modeling in disturbed environments using remote sensing

Importantly, the temperature models of this study built purely from remote sensing metrics had similar goodness-of-fit metrics to monthly microclimate models built using a combination of field and remote-sensing data (Greiser et al., 2018). Further, the observed coefficients of determination between canopy height and mean growing season temperatures align with prior work, where tree canopy explains about 20 % of the difference between open-air and below tree canopy temperatures (Thom et al., 2020). In the context of this prior research, my

findings suggest that remote-sensing metrics can be utilized to improve our microclimate modeling capacity (Zellweger et al., 2019).

I observed variability in model explanatory power across months of the growing season. Early and late season monthly models of temperature had higher explanatory power compared to growing season models. The lower explanatory power for growing season models and models of July and August could be a result of differences in the near-surface environment in these months – particularly increased dominance of understory cover (Prévosto et al., 2020). From mid-June to late August fireweed (*Epilobium angustifolium*), a tall (0.5 – 1.5 m) perennial plant, dominates burned environments at AFRF. Canopy height models did not incorporate any vegetation below 2 m, thus the impact of fireweed or any other understory cover would not be captured. Mid-summer understory dominance could explain the decreased goodness-of-fit mid-summer and the overall lower model fit for growing season models.

I found differences in canopy structure (a difference of ~ 5 m in canopy height) resulting from a fire disturbance are associated with large changes in microclimate conditions. These relatively small differences in canopy height that correspond to large changes in microclimate are a globally consistent trend (Baker et al., 2014; Davis et al., 2019b; Kermavnar et al., 2020) and such canopy changes can impair successful post-burn establishment in western North American forests. Forest managers should consider the impact of a minor disturbance or small differences in canopy height when modeling ecosystem processes that are influenced by microclimate conditions (McDowell et al., 2020; Park Williams et al., 2013).

Chapter 4: Conclusions

4.1 Overarching goal of research: relationship between disturbed canopy and microclimate

The overarching goal of this research study was to investigate the relationship between tree canopy and microclimate in a burned forest. A literature review defined the need and the scope for this work by outlining microclimate dynamics, with a focus on the impact of forest canopy on microclimate and the importance of spatial resolution for improving microclimate modeling.

The literature review identified a need to clarify what scale of spatial buffer is necessary for incorporating microclimate drivers. I considered defining this scale of buffer a precursor to later modeling. Following this identification, the first analysis in Chapter 3 determined the buffer of canopy height with the strongest correlation to microclimate measurements for use in later models. Soil moisture models improved accuracy when summarizing canopy height at fine scales, but coefficients of determination were overall low for these models. Conversely, canopy height summarized with buffer at a larger scale (15m) had a higher correlation with mean growing season temperature. The use of larger scales for temperature modeling is a key outcome of this work as lower resolution data decreases the processing times and cost associated with deriving metrics used for microclimate modeling (Zellweger et al., 2019).

After identifying the scale of spatial buffer to describe the influence of canopy height, the second analysis in Chapter 3 characterized the relationship between canopy height and microclimate during the whole growing season and across months. Growing season and monthly models used canopy height summarized with a larger buffer for temperatures and a smaller buffer for soil moisture. There was strong support for the impact of canopy height on growing season and monthly mean temperatures. Taller canopies, which also had more canopy cover,

were associated with cooler and less variable microclimate temperatures than short canopies. The estimate of the slope coefficient associated with canopy height for soil temperatures was double in magnitude compared to surface measurements, supporting that the presence of a healthy tree canopy strongly cooled soil temperatures. Additionally, the impact of canopy height differed throughout the months of the growing season, suggesting that adjusted gridded climate models should integrate microclimate correction factors that fluctuate throughout seasons. Soil moisture models suggested a weak negative relationship between taller canopies and drier locations.

Overall, my study shows that small differences in disturbed forest canopies result in large changes in microclimate variables, particularly soil temperatures, at both growing season and monthly scales. In particular, in contrast to past research, I found soil temperature is strongly affected by differences in the canopy (Ashcroft and Gollan, 2013) – which is known to impact seedling regeneration (Hansen and Turner, 2019). I argue that climate conditions differ in a post-disturbance forest mainly due to relatively small differences (~ 5 m) in canopy height, which is correlated to canopy cover in this environment. To expedite future microclimate research, I define the spatial buffer necessary for incorporating the impact of canopy on soil moisture and temperature variables. Canopy height better explained soil moisture with small or fine buffers and temperature with larger buffers. Importantly, I found microclimate conditions varied widely in a relatively small area with similar pre-fire habitats and that microclimate conditions were correlated to metrics of canopy structure. Thus, a fire disturbance can result in changes in the overall climate and buffering capacity of near-ground environments that tree seedlings inhabit.

4.2 Importance of research and key findings

This research project was possible due to a rapid expansion of new technology to measure canopy and topography and collect in-situ measurements of microclimate. Such technological development allows us to accurately model microclimate dynamics in many

different environments at successional stages. Models of microclimate dynamics can assist the development of correction factors for known microclimate drivers, including topography and canopy, that are then input into gridded microclimate models (Zellweger et al., 2019). Prior work argues that sub-meter resolution data are necessary for developing correction factors for known microclimate drivers (Lenoir et al., 2017). However, these sub-meter datasets have a high time and cost intensity (Zellweger et al., 2019).

A key finding of the current work is that the impact of a forest canopy on microclimate temperature may be better modeled with moderate spatial resolution (> 15 m) forest structure metrics. This has relevance for addressing a need for global maps of microclimate conditions (De Frenne et al., 2021). The spatial resolutions with the strongest correlation to growing season temperature – 15 meters – suggest microclimate modelers could rely on space-based sensors for measurements of global forest structure, as these instruments can have resolutions as fine as 25 m (Qi et al., 2019). In particular, the Global Ecosystem Dynamics Investigation (GEDI) is an openly available space-based LiDAR product that produces forest structure metrics including canopy height and LAI at a 25 m resolution. Given differences in correlation between 15 and 20 m in the present study were small, space-based metrics of canopy could be integrated with work to produce accurate gridded microclimate datasets (Qi et al., 2019).

Another key outcome of this work is soil moisture measurements were not strongly impacted by differences in canopy height nor well explained by high-resolution metrics of elevation, aspect, and tree canopy. Mixed effect models, that included elevation and aspect, supported that the variation in soil moisture as explained by all remote-sensing-based metrics was small. This finding contrasts past work in Tundra regions, where an elevation range as small as 200 m was a strong determinant of soil moisture, but these Tundra regions are less influenced by transpiration and canopy interception (Kempainen et al., 2018). In the fire disturbed forests of

western North America, research supports soil moisture dynamics are not well described by canopy loss (Goeking and Tarboton, 2020), suggesting a need for further research on the drivers of soil moisture across different ecosystems. Differences among locations like canopy species composition, shrub-layers, and bedrock topography influence temporal and spatial soil moisture measurements, because they impact evapotranspiration and rates of water flow (Dingman, 2015).

Expanding our capacity to build microclimate maps across broad spatial scales includes differentiating between disturbed and non-disturbed forests. This study showed that areas with lower canopy heights, which correlated to overall canopy condition, had different microclimates compared to taller canopies, particularly for soil temperature. A recent meta-analysis on the difference between soil and air temperatures supports a significant deviance between air and soil temperature, but the direction of deviance is variable by biome type, where cool and wet biomes have warmer soils, and hot and dry biomes are opposite with slightly cooler soils (Lembrechts et al., 2021b). In the present study, differences in canopy height were one of the strongest determinants of soil temperatures. Thus, differences in canopy height that are a result of a fire could change the buffering capacity of these disturbed forests. At this northern latitude, this would switch the direction of soil temperature buffering from warmer mean annual soil temperature to cooler annual soil temperatures (Greiser et al., 2018).

4.3 Limitations of research

4.3.1 Assumptions of the study design

This project sampled within the growing season at AFRF, but many studies support that the patterns of canopy buffering differs as a function of season, where locations beneath forest canopies are generally cooler in summer and warmer in winter (Ashcroft and Gollan, 2013; Greiser et al., 2018; von Arx et al., 2012). The study is limited in that it can only make inferences on microclimate dynamics relevant to the AFRF growing season. However, studies of

regeneration support that the growing season microclimates influence successful regeneration (Hansen and Turner, 2019; North et al., 2019; Stevens-Rumann et al., 2018). Thus, my findings of growing season microclimate are applicable when considering forest regeneration.

The study design is also limited because it assumes differences in microclimate explained by canopy height are not a result of harvest history or forest type. In my site selection, I placed forest plots in wildlife tree patches, which are areas preserved from logging, and similar pre-fire environments as defined by the site descriptions of AFRF (Klinka et al., 2004). However, the realities of working in harvested forests resulted in likely edge-effects, which some research suggests extend as far as 100 m into the forest (Klinka et al., 2004). Further, while plots were limited to similar pre-fire environments, I did not measure pre-fire stand development. Prior estimates of pre-fire tree height was similar for most plots, with the exception of one plot in an older forest (Klinka et al., 2004). Importantly, I acknowledge that the observed differences in microclimate could also promote forest growth, exacerbating the observed differences in canopy height. My study is a snapshot of the impact of forest structure that supports canopy height is correlated with differences in microclimate.

I acknowledge that the focus on tree canopy height limits the conclusions drawn from this work. However, I found no difference in the overall model fit using canopy cover as an explanatory variable. This is likely because my measurements of canopy height were strongly correlated with metrics of canopy cover (Figure S8). I argue canopy height can improve microclimate modeling because prior research has also found that it a strong predictor of microclimate (Jucker et al., 2018), and across the gradient of burned forest plots, canopy height correlates to measurements of canopy cover, another microclimate drivers (Figure S8). Importantly, this study does not address the impact of understory vegetation cover or structure, which is important to consider for microclimate modeling (Prévosto et al., 2020)

4.3.2 Measurement error

The structure of TMS-4 sensors may have introduced inaccuracies in my research. Although field-based studies support that the TMS-4 sensors are accurate within 0.5 °C (Wild et al., 2019), ground surface reflectance onto the solar shields can increase temperature measurements (Ashcroft and Gollan, 2012). Ground reflectance would increase temperatures recorded for the near-surface and surface sensors in areas that receive intense solar radiation. It could also result in raised soil temperatures and increased evapotranspiration (Oke, 2002). Errors in these measurements are a broader problem of microclimate measurements (Maclean et al., 2021), and consideration of these errors, while important, is generally out-of-scope for the current work. Additionally, as these errors are present across all global studies (De Frenne et al., 2019), our results can be considered consistent with this broader global context.

I must also acknowledge inaccuracies in my remote-sensing metrics, namely that the canopy height model overestimated low canopy height values (Appendix C). Overestimation is likely due to the inclusion of dead and sub-canopy trees that are difficult to capture in DAP models (Graham, 2019). The DAP model captured the tallest tree height, but as canopy height was averaged over a 6.5 radius, the lack of a tree crown in burned areas skewed the DAP model to overpredict tree height. Many DAP pixels had low height values because burned trees had no crown. When both locations in severely burnt crowns and the one location with a dominance of sub-canopy trees were removed, the model fit was improved ($R^2 = 0.82$) and fit a one-to-one line (slope = 1.0 $p \ll 0.05$, intercept = 0.1 $p > 0.5$). In this case, discrepancies between the DAP and field heights are mostly a result of the tree form (Vauhkonen et al., 2012, Figure S7). While this is an inaccuracy, my DAP-derived heights may better represent the ultimate impact on microclimate, because they better describe the form of tree crowns and are strongly correlated with estimates of cover (Vauhkonen et al., 2012, Figure S8).

4.4 Future work

4.4.1 Analyses utilizing the thesis dataset

The dataset produced in companion to this thesis provides a high density of temperature and moisture measurements per unit area. In the global “soil temperature database,” there are currently ten other locations with similar densities of soil temperature measurements per unit area (Lembrechts et al., 2021b). As a result, this dataset offers many future research possibilities. Perhaps most of interest to microclimate modelers is how my field site's microclimate dynamics compare to downscaled climate models. In this case, gridded climate datasets could be downscaled using spatial data (canopy and topography metrics) and compared to in-situ measurements. Lembrechts et al. (2019) completed a similar study that compared in-situ to four gridded climate models in northern Scandinavia. They found in-situ measurements consistently outperformed downscaled gridded climate models, but there was variable measurement accuracy gained by downscaling a dataset from 1 km to 30 m (Lembrechts et al., 2019).

A recent review on microclimate supports a need to create accurate correction factors for canopy and topography to downscaled gridded climate models and improve alignment to in-situ measurements (De Frenne et al., 2021). Satellite-based remote sensing products like ICESat and GEDI can enhance the current dataset and expand future directions (Qi et al., 2019). For example, a comparison of model accuracy using RPA and space-borne estimates of canopy height or canopy cover would be a valuable investigation for methods to advance global microclimate modeling and downscaling climate measurements (De Frenne et al., 2021).

In addition to the remote-sensing metrics, field data could also be investigated to model AFRF microclimate dynamics. This thesis worked principally with remote-sensing metrics, but this dataset also includes soil type, litter depth, understory vegetation data, and leaf area index data (Appendix D). In open landscapes, like those in high burn severity, understory vegetation

plays a large role in buffering from extreme temperatures and decreasing vapor pressure deficit (Prévosto et al., 2020). Expanding on the current work at monthly and growing-season timesteps, diurnal microclimate models could be built using a combination of field and remote-sensing data. Diurnal models could investigate the relative impact of different vegetation types, including the understory structure, litter depth, and tree canopy. Diurnal climate models are important for modeling fire ignition risk, and knowledge of the impact of vegetation could help inform successful fire risk mitigation (Costafreda-Aumedes et al., 2018).

4.4.2 Expansion of microclimate research at a global scale

To expand on the research on microclimate in disturbed forests globally, future work should measure microclimate in relation to forest canopy in all seasons and across years. This project is a snapshot of the impact of canopy height on microclimate during the growing season, but further research in different ecosystems is necessary to clarify the impact of canopy height. Studies in the southwestern United States support that tree canopy influences rates of snow-deposition, which produces differing spring soil moisture (Harpold et al., 2014). Further, snow deposition is known to decouple or create entirely different surface and soil temperature dynamics (Oke, 2002). To accurately adjust gridded climate datasets, calibration and correction factors must be accurate to the system and the season, which requires research to expand beyond the growing season alone. It additionally requires the expansion of microclimate studies in diverse locales, particularly in disturbed environments, as these represent the locations most likely to have dramatic ecosystem shifts (McDowell et al., 2020).

References

- Agisoft, L.L.C., 2018. Agisoft Metashape User Manual - Professional Edition, Version 1.5.
- Anderson, P.D., Larson, D.J., Chan, S.S., 2007. Riparian buffer and density management influences on microclimate of young headwater forests of western oregon. *Forest Science* 53, 254–269. <https://doi.org/10.1093/forestscience/53.2.254>
- Andrade, A.J., Tomback, D.F., Seastedt, T.R., Mellmann-Brown, S., 2021. Soil moisture regime and canopy closure structure subalpine understory development during the first three decades following fire. *Forest Ecology and Management* 483, 118783. <https://doi.org/10.1016/j.foreco.2020.118783>
- Arkin, J., Coops, N.C., Hermosilla, T., Daniels, L.D., Plowright, A., 2019. Integrated fire severity–land cover mapping using very-high-spatial-resolution aerial imagery and point clouds. *International Journal of Wildland Fire*. <https://doi.org/10.1071/WF19008>
- Ashcroft, M.B., Gollan, J.R., 2013. Moisture, thermal inertia, and the spatial distributions of near-surface soil and air temperatures: Understanding factors that promote microrefugia. *Agricultural and Forest Meteorology* 176, 77–89. <https://doi.org/10.1016/j.agrformet.2013.03.008>
- Ashcroft, M.B., Gollan, J.R., 2012. Fine-resolution (25 m) topoclimatic grids of near-surface (5 cm) extreme temperatures and humidities across various habitats in a large (200 × 300 km) and diverse region. *International Journal of Climatology* 32, 2134–2148. <https://doi.org/10.1002/joc.2428>
- Ashcroft, M.B., Gollan, J.R., Warton, D.I., Ramp, D., 2012. A novel approach to quantify and locate potential microrefugia using topoclimate, climate stability, and isolation from the matrix. *Global Change Biology* 18, 1866–1879. <https://doi.org/10.1111/j.1365-2486.2012.02661.x>
- ASTM Committee D-18 on Soil and Rock, 2017. Standard practice for classification of soils for engineering purposes. ASTM International.
- Baker, T.P., Jordan, G.J., Steel, E.A., Fountain-Jones, N.M., Wardlaw, T.J., Baker, S.C., 2014. Microclimate through space and time: microclimatic variation at the edge of regeneration forests over daily, yearly and decadal time scales. *Forest Ecology and Management* 334, 174–184. <https://doi.org/10.1016/j.foreco.2014.09.008>
- Bates, D., Mächler, M., Bolker, B., Walker, S., 2015. fitting linear mixed-effects models using lme4. arXiv preprint arXiv:1406.5823.
- Beudert, B., Bässler, C., Thorn, S., Noss, R., Schröder, B., Dieffenbach-Fries, H., Foullois, N., Müller, J., 2015. Bark beetles increase biodiversity while maintaining drinking water quality. *Conservation Letters* 8, 272–281. <https://doi.org/10.1111/conl.12153>
- Biederman, J.A., Somor, A.J., Harpold, A.A., Gutmann, E.D., Breshears, D.D., Troch, P.A., Gochis, D.J., Scott, R.L., Meddens, A.J.H., Brooks, P.D., 2017. Recent tree die-off has little effect on streamflow in contrast to expected increases from historical studies. *Water Resources Research* 51(12), 9775–9789. <https://doi.org/10.1002/2015WR017401>
- Blonder, B., Both, S., Coomes, D.A., Elias, D., Jucker, T., Kvasnica, J., Majalap, N., Malhi, Y.S., Milodowski, D., Riutta, T., Svátek, M., 2018. Extreme and highly heterogeneous microclimates in selectively logged tropical forests. *Frontiers in Forests and Global Change* 1, 5. <https://doi.org/10.3389/ffgc.2018.00005>

- Braziunas, K.H., Hansen, W.D., Seidl, R., Rammer, W., Turner, M.G., 2018. Looking beyond the mean: Drivers of variability in postfire stand development of conifers in Greater Yellowstone. *Forest Ecology and Management* 430, 460–471. <https://doi.org/10.1016/j.foreco.2018.08.034>
- Breshears, D.D., Rich, P.M., Barnes, F.J., Campbell, K., 1997. Overstory-imposed heterogeneity in solar radiation and soil moisture in a semiarid woodland. *Ecological Applications* 7(4), 1201–1215. [https://doi.org/10.1890/1051-0761\(1997\)007\[1201:OIHISR\]2.0.CO;2](https://doi.org/10.1890/1051-0761(1997)007[1201:OIHISR]2.0.CO;2)
- Chen, J., Saunders, S.C., Crow, T.R., Naiman, R.J., Brosofske, K.D., Mroz, G.D., Brookshire, B.L., Franklin, J.F., 1999. Microclimate in forest ecosystem and landscape ecology variations in local climate can be used to monitor and compare the effects of different management regimes. *BioScience* 49(4), 288–297. <https://doi.org/10.2307/1313612>
- Chen, X., Vogelmann, J.E., Rollins, M., Ohlen, D., Key, C.H., Yang, L., Huang, C., Shi, H., 2011. Detecting post-fire burn severity and vegetation recovery using multitemporal remote sensing spectral indices and field-collected composite burn index data in a ponderosa pine forest. *International Journal of Remote Sensing* 32(23), 7905–7927. <https://doi.org/10.1080/01431161.2010.524678>
- Chisholm, R.A., Cui, J., Lum, S.K.Y., Chen, B.M., 2013. UAV LiDAR for below-canopy forest surveys. *Journal of Unmanned Vehicle Systems* 1(01), 61–68. <https://doi.org/10.1139/juvs-2013-0017>
- Clark, K.L., Skowronski, N.S., Gallagher, M.R., Renninger, H., Schäfer, K.V.R., 2014. Contrasting effects of invasive insects and fire on ecosystem water use efficiency. *Biogeosciences* 11(23), 6509–6523. <https://doi.org/10.5194/bg-11-6509-2014>
- CloudCompare, 2020.
- Colomina, I., Molina, P., 2014. Unmanned aerial systems for photogrammetry and remote sensing: A review. *ISPRS Journal of Photogrammetry and Remote Sensing* 92, 79–97. <https://doi.org/10.1016/j.isprsjprs.2014.02.013>
- Coops, N.C., Duffe, J., Koot, C., 2010. Assessing the utility of lidar remote sensing technology to identify mule deer winter habitat. *Canadian Journal of Remote Sensing* 36(2), 81–88. <https://doi.org/10.5589/m10-029>
- Costafreda-Aumedes, S., Comas, C., Vega-Garcia, C., Costafreda-Aumedes, S., Comas, C., Vega-Garcia, C., 2018. Human-caused fire occurrence modelling in perspective: a review. *International Journal of Wildland Fire* 26(12), 983–998. <https://doi.org/10.1071/WF17026>
- Dai, W., Goodale, E., He, R., Mammides, C., Liu, S., Zhou, L., Tang, S., Su, B., Lao, X., Jiang, A., 2021. An eco-compensation policy increases shorebird diversity during the non-farming period for aquaculture. *Wetlands* 41(1), 4. <https://doi.org/10.1007/s13157-021-01397-7>
- Daly, C., Halbleib, M., Smith, J.I., Gibson, W.P., Doggett, M.K., Taylor, G.H., Curtis, J., Pasteris, P.P., 2008. Physiographically sensitive mapping of climatological temperature and precipitation across the conterminous United States. *International Journal of Climatology* 28(15), 2031–2064. <https://doi.org/10.1002/joc.1688>
- Davis, K.T., Dobrowski, S.Z., Higuera, P.E., Holden, Z.A., Veblen, T.T., Rother, M.T., Parks, S.A., Sala, A., Maneta, M.P., 2019a. Wildfires and climate change push low-elevation forests across a critical climate threshold for tree regeneration. *PNAS* 116(13), 6193–6198. <https://doi.org/10.1073/pnas.1815107116>

- Davis, K.T., Dobrowski, S.Z., Holden, Z.A., Higuera, P.E., Abatzoglou, J.T., 2019b. Microclimatic buffering in forests of the future: The role of local water balance. *Ecography* 42(1), 1–11. <https://doi.org/10.1111/ecog.03836>
- de Almeida, D.R.A., Stark, S.C., Valbuena, R., Broadbent, E.N., Silva, T.S.F., de Resende, A.F., Ferreira, M.P., Cardil, A., Silva, C.A., Amazonas, N., Zambrano, A.M.A., Brancalion, P.H.S., 2020. A new era in forest restoration monitoring. *Restoration Ecology* 28(1), 8–11. <https://doi.org/10.1111/rec.13067>
- De Frenne, P., Lenoir, J., Luoto, M., Scheffers, B.R., Zellweger, F., Aalto, J., Ashcroft, M.B., Christiansen, D.M., Decocq, G., Pauw, K.D., Govaert, S., Greiser, C., Gril, E., Hampe, A., Jucker, T., Klinges, D.H., Koelemeijer, I.A., Lembrechts, J.J., Marrec, R., Meeussen, C., Ogée, J., Tyystjärvi, V., Vangansbeke, P., Hylander, K., 2021. Forest microclimates and climate change: Importance, drivers and future research agenda. *Global Change Biology* 27(11), 2279–2297. <https://doi.org/10.1111/gcb.15569>
- De Frenne, P., Zellweger, F., Rodríguez-Sánchez, F., Scheffers, B.R., Hylander, K., Luoto, M., Vellend, M., Verheyen, K., Lenoir, J., 2019. Global buffering of temperatures under forest canopies. *Nature Ecology & Evolution* 3(5), 744–749. <https://doi.org/10.1038/s41559-019-0842-1>
- Di Stefano, J., 2004. A confidence interval approach to data analysis. *Forest Ecology and Management* 187(2-3), 173–183. [https://doi.org/10.1016/S0378-1127\(03\)00331-1](https://doi.org/10.1016/S0378-1127(03)00331-1)
- Dietmaier, A., McDermid, G.J., Rahman, M.M., Linke, J., Ludwig, R., 2019. Comparison of LiDAR and digital aerial photogrammetry for characterizing canopy openings in the boreal forest of northern Alberta. *Remote Sensing* 11(16), 1919. <https://doi.org/10.3390/rs11161919>
- Dietz, L., Collet, C., Dupouey, J.-L., Lacombe, E., Laurent, L., Gégout, J.-C., 2020. Windstorm-induced canopy openings accelerate temperate forest adaptation to global warming. *Global Ecology and Biogeography* 29(11), 2067–2077. <https://doi.org/10.1111/geb.13177>
- Dingman, J.R., Sweet, L.C., McCullough, I., Davis, F.W., Flint, A., Franklin, J., Flint, L.E., 2013. Cross-scale modeling of surface temperature and tree seedling establishment in mountain landscapes. *Ecological Processes* 2(1), 30. <https://doi.org/10.1186/2192-1709-2-30>
- Dingman, S.L., 2015. *Physical Hydrology: Third Edition*. Waveland Press.
- DJI GS RTK App, 2020. DJI.
- Dormann, C.F., Elith, J., Bacher, S., Buchmann, C., Carl, G., Carré, G., Marquéz, J.R.G., Gruber, B., Lafourcade, B., Leitão, P.J., Münkemüller, T., McClean, C., Osborne, P.E., Reineking, B., Schröder, B., Skidmore, A.K., Zurell, D., Lautenbach, S., 2013. Collinearity: a review of methods to deal with it and a simulation study evaluating their performance. *Ecography* 36(1), 27–46. <https://doi.org/10.1111/j.1600-0587.2012.07348.x>
- Eskelson, B.N.I., Anderson, P.D., Hagar, J.C., Temesgen, H., 2011. Geostatistical modeling of riparian forest microclimate and its implications for sampling. *Canadian Journal of Forest Research*, 41(5), 974–985. <https://doi.org/10.1139/x11-015>
- Feduck, C., McDermid, G., Castilla, G., Feduck, C., McDermid, G.J., Castilla, G., 2018. Detection of coniferous seedlings in UAV imagery. *Forests* 9(7), 432. <https://doi.org/10.3390/f9070432>

- Frey, S.J.K., Hadley, A.S., Johnson, S.L., Schulze, M., Jones, J.A., Betts, M.G., 2016. Spatial models reveal the microclimatic buffering capacity of old-growth forests. *Science Advances* 2(4), e1501392. <https://doi.org/10.1126/sciadv.1501392>
- Frolking, S., Palace, M.W., Clark, D.B., Chambers, J.Q., Shugart, H.H., Hurtt, G.C., 2009. Forest disturbance and recovery: A general review in the context of spaceborne remote sensing of impacts on aboveground biomass and canopy structure. *Journal of Geophysical Research-Biogeosciences*. 114(G2), G00E02. <https://doi.org/10.1029/2008JG000911>
- Fuka, D.R., Collick, A.S., Kleinman, P.J.A., Auerbach, D.A., Harmel, R.D., Easton, Z.M., 2016. Improving the spatial representation of soil properties and hydrology using topographically derived initialization processes in the SWAT model. *Hydrological Processes* 30(24), 4633–4643. <https://doi.org/10.1002/hyp.10899>
- Geiger, R., 1950. *The Climate Near The Ground*. Harvard University Press.
- Gendreau-Berthiaume, B., Macdonald, S.E., Stadt, J.J., 2018. Importance of the canopy in determining on-going regeneration and stand successional development in lodgepole pine forests. *Journal of Vegetation Science* 29(2), 213–225. <https://doi.org/10.1111/jvs.12622>
- Goeking, S.A., Tarboton, D.G., 2020. Forests and water yield: A synthesis of disturbance effects on streamflow and snowpack in western coniferous forests. *Journal of Forestry* 118(2), 172–192. <https://doi.org/10.1093/jofore/fvz069>
- Goodbody, T.R.H., 2019. Assessing the role of digital aerial photogrammetry for characterizing forest structure and enhancing forest inventories. University of British Columbia. <https://doi.org/10.14288/1.0376651>
- Goodbody, T.R.H., Coops, N.C., White, J.C., 2019. Digital aerial photogrammetry for updating area-based forest inventories: A review of opportunities, challenges, and future directions. *Current Forestry Reports* 5(2), 55–75. <https://doi.org/10.1007/s40725-019-00087-2>
- Graham, A., Coops, N.C., Wilcox, M., Plowright, A., 2019. Evaluation of Ground Surface Models Derived from Unmanned Aerial Systems with Digital Aerial Photogrammetry in a Disturbed Conifer Forest. *Remote Sensing* 11(1), 84. <https://doi.org/10.3390/rs11010084>
- Graham, A.N.V., 2019. Assessing terrain modelling and forest inventory capabilities of digital aerial photogrammetry from autonomous aerial systems. University of British Columbia. <https://doi.org/10.14288/1.0380670>
- Greiser, C., Meineri, E., Luoto, M., Ehrlén, J., Hylander, K., 2018. Monthly microclimate models in a managed boreal forest landscape. *Agricultural and Forest Meteorology* 250–251, 147–158. <https://doi.org/10.1016/j.agrformet.2017.12.252>
- Halama, J.J., Barnhart, B.L., Kennedy, R.E., McKane, R.B., Graham, J.J., Pettus, P.P., Brookes, A.F., Djang, K.S., Waschmann, R.S., 2018. Improved soil temperature modeling using spatially explicit solar energy drivers. *Water* 10(10), 1398. <https://doi.org/10.3390/w10101398>
- Hansen, W.D., Turner, M.G., 2019. Origins of abrupt change? Postfire subalpine conifer regeneration declines nonlinearly with warming and drying. *Ecological Monographs* 89(1), e01340. <https://doi.org/10.1002/ecm.1340>
- Hardwick, S.R., Toumi, R., Pfeifer, M., Turner, E.C., Nilus, R., Ewers, R.M., 2015. The relationship between leaf area index and microclimate in tropical forest and oil palm

- plantation: Forest disturbance drives changes in microclimate. *Agricultural and Forest Meteorology* 201, 187–195. <https://doi.org/10.1016/j.agrformet.2014.11.010>
- Harpold, A.A., Biederman, J.A., Condon, K., Merino, M., Korgaonkar, Y., Nan, T., Sloat, L.L., Ross, M., Brooks, P.D., 2014. Changes in snow accumulation and ablation following the Las Conchas Forest Fire, New Mexico, USA. *Ecohydrology* 7(2), 440–452. <https://doi.org/10.1002/eco.1363>
- Haughian, S.R., Burton, P.J., 2018. Microclimate differences above ground-layer vegetation in lichen-dominated pine forests of north-central British Columbia. *Agricultural and Forest Meteorology* 249, 100–106. <https://doi.org/10.1016/j.agrformet.2017.11.029>
- Heithecker, T.D., Halpern, C.B., 2007. Edge-related gradients in microclimate in forest aggregates following structural retention harvests in western Washington. *Forest Ecology and Management* 248(3), 163–173. <https://doi.org/10.1016/j.foreco.2007.05.003>
- Hijmans, R., Van Etten, J., Cheng, J., Mattiuzzi, M., Sumner, M., Greenberg, J., Perpinan Lamigueiro, O., 2015. Package “raster”: Geographic analysis and modeling with raster data.
- Hoecker, T.J., Hansen, W.D., Turner, M.G., 2020. Topographic position amplifies consequences of short-interval stand-replacing fires on postfire tree establishment in subalpine conifer forests. *Forest Ecology and Management* 478, 118523. <https://doi.org/10.1016/j.foreco.2020.118523>
- Hope, E.S., McKenney, D.W., Pedlar, J.H., Stocks, B.J., Gauthier, S., 2016. Wildfire suppression costs for Canada under a changing climate. *PLOS ONE* 11(8), e0157425. <https://doi.org/10.1371/journal.pone.0157425>
- Jucker, T., Bongalov, B., Burslem, D.F.R.P., Nilus, R., Dalponte, M., Lewis, S.L., Phillips, O.L., Qie, L., Coomes, D.A., 2018a. Topography shapes the structure, composition and function of tropical forest landscapes. *Ecology Letters* 21(7), 989–1000. <https://doi.org/10.1111/ele.12964>
- Jucker, T., Hardwick, S.R., Both, S., Elias, D.M.O., Ewers, R.M., Milodowski, D.T., Swinfield, T., Coomes, D.A., 2018b. Canopy structure and topography jointly constrain the microclimate of human-modified tropical landscapes. *Global Change Biology* 24(11), 5243–5258. <https://doi.org/10.1111/gcb.14415>
- Kemppinen, J., Niittynen, P., Riihimäki, H., Luoto, M., 2018. Modelling soil moisture in a high-latitude landscape using LiDAR and soil data. *Earth Surface Processes and Landforms* 43(5), 1019–1031. <https://doi.org/10.1002/esp.4301>
- Kermavnar, J., Ferlan, M., Marinšek, A., Eler, K., Kobler, A., Kutnar, L., 2020. Effects of various cutting treatments and topographic factors on microclimatic conditions in Dinaric fir-beech forests. *Agricultural and Forest Meteorology* 295, 108186. <https://doi.org/10.1016/j.agrformet.2020.108186>
- Klinka, K., Varga, P., Koot, C., Rau, M., Macku, J., Kusbach, T., 2004. Site units of the University of British Columbia Alex Fraser research forest. University of British Columbia, Alex Fraser Research Forest.
- Kovács, B., Tinya, F., Ódor, P., 2017. Stand structural drivers of microclimate in mature temperate mixed forests. *Agricultural and Forest Meteorology* 234–235, 11–21. <https://doi.org/10.1016/j.agrformet.2016.11.268>
- Laamrani, A., Valeria, O., Bergeron, Y., Fenton, N., Cheng, L.Z., Anyomi, K., 2014. Effects of topography and thickness of organic layer on productivity of black spruce boreal forests

- of the Canadian Clay Belt region. *Forest Ecology and Management* 330, 144–157.
<https://doi.org/10.1016/j.foreco.2014.07.013>
- Latimer, C.E., Zuckerberg, B., 2017. Forest fragmentation alters winter microclimates and microrefugia in human-modified landscapes. *Ecography* 40(1), 158–170.
<https://doi.org/10.1111/ecog.02551>
- Lazarus, B.E., Castanha, C., Germino, M.J., Kueppers, L.M., Moyes, A.B., 2018. Growth strategies and threshold responses to water deficit modulate effects of warming on tree seedlings from forest to alpine. *Journal of Ecology* 106(2), 571–585.
<https://doi.org/10.1111/1365-2745.12837>
- Legendre-Fixx, M., Anderegg, L.D.L., Ettinger, A.K., HilleRisLambers, J., 2018. Site- and species-specific influences on sub-alpine conifer growth in Mt. Rainier National Park, USA. *Forests* 9(1), 1. <http://dx.doi.org/10.3390/f9010001>
- Leica Geosystems, 2020. Measurement Performance & Accuracy [WWW Document]. Leica Viva GNSS GS14 receiver Datasheet.
- Lembrechts, J.J., Aalto, J., Ashcroft, M.B., Frenne, P.D., Kopecký, M., Lenoir, J., Luoto, M., Maclean, I.M.D., Roupsard, O., Fuentes-Lillo, E., García, R.A., Pellissier, L., Pitteloud, C., Alatalo, J.M., Smith, S.W., Björk, R.G., Muffler, L., Backes, A.R., Cesarz, S., Gottschall, F., Okello, J., Urban, J., Plichta, R., Svátek, M., Phartyal, S.S., Wipf, S., Eisenhauer, N., Puşcaş, M., Turtureanu, P.D., Varlagin, A., Dimarco, R.D., Jump, A.S., Randall, K., Dorrepaal, E., Larson, K., Walz, J., Vitale, L., Svoboda, M., Higgins, R.F., Halbritter, A.H., Curasi, S.R., Klupar, I., Koontz, A., Pearse, W.D., Simpson, E., Stemkovski, M., Graae, B.J., Sørensen, M.V., Høye, T.T., Calzado, M.R.F., Lorite, J., Carbognani, M., Tomaselli, M., Forte, T.G.W., Petraglia, A., Haesen, S., Somers, B., Meerbeek, K.V., Björkman, M.P., Hylander, K., Merinero, S., Gharun, M., Buchmann, N., Dolezal, J., Matula, R., Thomas, A.D., Bailey, J.J., Ghosn, D., Kazakis, G., Pablo, M.A. de, Kempainen, J., Niittynen, P., Rew, L., Seipel, T., Larson, C., Speed, J.D.M., Ardö, J., Cannone, N., Guglielmin, M., Malfasi, F., Bader, M.Y., Canessa, R., Stanisci, A., Kreyling, J., Schmeddes, J., Teuber, L., Aschero, V., Čiliak, M., Máliš, F., Smedt, P.D., Govaert, S., Meeussen, C., Vangansbeke, P., Gigauri, K., Lamprecht, A., Pauli, H., Steinbauer, K., Winkler, M., Ueyama, M., Nuñez, M.A., Ursu, T.-M., Haider, S., Wedegärtner, R.E.M., Smiljanic, M., Trouillier, M., Wilmking, M., Altman, J., Bruna, J., Hederová, L., Macek, M., Man, M., Wild, J., Vittoz, P., Pärtel, M., Barančok, P., Kanka, R., Kollár, J., Palaj, A., Barros, A., Mazzolari, A.C., Bauters, M., Boeckx, P., Alonso, J.-L.B., Zong, S., Cecco, V.D., Sitková, Z., Tielbörger, K., Brink, L. van den, Weigel, R., Homeier, J., Dahlberg, C.J., Medinets, S., Medinets, V., Boeck, H.J.D., Portillo-Estrada, M., Verryckt, L.T., Milbau, A., Daskalova, G.N., Thomas, H.J.D., Myers-Smith, I.H., Blonder, B., Stephan, J.G., Descombes, P., Zellweger, F., Frei, E.R., Heinesch, B., Andrews, C., Dick, J., Siebicke, L., Rocha, A., Senior, R.A., Rixen, C., Jimenez, J.J., Boike, J., Pauchard, A., Scholten, T., Scheffers, B., Klinges, D., Basham, E.W., Zhang, J., Zhang, Z., Géron, C., Fazlioglu, F., Candan, O., Bravo, J.S., Hrbacek, F., Laska, K., Cremonese, E., Haase, P., Moyano, F.E., Rossi, C., Nijs, I., 2020. SoilTemp: A global database of near-surface temperature. *Global Change Biology* 26, 6616–6629.
<https://doi.org/10.1111/gcb.15123>
- Lembrechts, J.J., Lenoir, J., Roth, N., Hattab, T., Milbau, A., Haider, S., Pellissier, L., Pauchard, A., Backes, A.R., Dimarco, R.D., Nuñez, M.A., Aalto, J., Nijs, I., 2019. Comparing

- temperature data sources for use in species distribution models: From in-situ logging to remote sensing. *Global Ecology and Biogeography* 28(11), 1578–1596. <https://doi.org/10.1111/geb.12974>
- Lembrechts, J.J., Lenoir, J., Scheffers, B.R., Frenne, P.D., 2021a. Designing countrywide and regional microclimate networks. *Global Ecology and Biogeography* 30(7), 1168–1174. <https://doi.org/10.1111/geb.13290>
- Lembrechts, J.J., van den Hoogen, J., Aalto, J., Ashcroft, M.B., De Frenne, P., Kimppinen, J., Lenoir, J., 2021b. Mismatches between soil and air temperature. <https://doi.org/10.32942/osf.io/pksqw>
- Lenoir, J., Hattab, T., Pierre, G., 2017. Climatic microrefugia under anthropogenic climate change: implications for species redistribution. *Ecography* 40(2), 253–266. <https://doi.org/10.1111/ecog.02788>
- Luo, W., Xu, X., Liu, W., Liu, M., Li, Z., Peng, T., Xu, C., Zhang, Y., Zhang, R., 2019. UAV based soil moisture remote sensing in a karst mountainous catchment. *CATENA* 174, 478–489. <https://doi.org/10.1016/j.catena.2018.11.017>
- Ma, S., Concilio, A., Oakley, B., North, M., Chen, J., 2010. Spatial variability in microclimate in a mixed-conifer forest before and after thinning and burning treatments. *Forest Ecology and Management* 259(5), 904–915. <https://doi.org/10.1016/j.foreco.2009.11.030>
- Maclean, I.M.D., 2020. Predicting future climate at high spatial and temporal resolution. *Global Change Biology* 26(2), 1003–1011. <https://doi.org/10.1111/geb.14876>
- Maclean, I.M.D., Duffy, J.P., Haesen, S., Govaert, S., Frenne, P.D., Vanneste, T., Lenoir, J., Lembrechts, J.J., Rhodes, M.W., Meerbeek, K.V., 2021. On the measurement of microclimate. *Methods in Ecology and Evolution* 00, 1–14. <https://doi.org/10.1111/2041-210X.13627>
- Maltamo, M., Næsset, E., Vauhkonen, J. (Eds.), 2014. *Forestry applications of airborne laser scanning: concepts and case studies, managing forest ecosystems*. Springer Netherlands, Dordrecht. <https://doi.org/10.1007/978-94-017-8663-8>
- McDowell, N.G., Allen, C.D., Anderson-Teixeira, K., Aukema, B.H., Bond-Lamberty, B., Chini, L., Clark, J.S., Dietze, M., Grossiord, C., Hanbury-Brown, A., Hurtt, G.C., Jackson, R.B., Johnson, D.J., Kueppers, L., Lichstein, J.W., Ogle, K., Poulter, B., Pugh, T.A.M., Seidl, R., Turner, M.G., Uriarte, M., Walker, A.P., Xu, C., 2020. Pervasive shifts in forest dynamics in a changing world. *Science* 368, 6494. <https://doi.org/10.1126/science.aaz9463>
- Miller, J.D., Thode, A.E., 2007. Quantifying burn severity in a heterogeneous landscape with a relative version of the delta Normalized Burn Ratio (dNBR). *Remote Sensing of Environment* 109(1), 66–80. <https://doi.org/10.1016/j.rse.2006.12.006>
- Nakagawa, S., Schielzeth, H., 2013. A general and simple method for obtaining R² from generalized linear mixed-effects models. *Methods in Ecology and Evolution* 4(2), 133–142. <https://doi.org/10.1111/j.2041-210x.2012.00261.x>
- North, M.P., Stevens, J.T., Greene, D.F., Coppoletta, M., Knapp, E.E., Latimer, A.M., Restaino, C.M., Tompkins, R.E., Welch, K.R., York, R.A., Young, D.J.N., Axelson, J.N., Buckley, T.N., Estes, B.L., Hager, R.N., Long, J.W., Meyer, M.D., Ostojka, S.M., Safford, H.D., Shive, K.L., Tubbesing, C.L., Vice, H., Walsh, D., Werner, C.M., Wyrsh, P., 2019. Tamm Review: Reforestation for resilience in dry western U.S. forests. *Forest Ecology and Management* 432, 209–224. <https://doi.org/10.1016/j.foreco.2018.09.007>

- Oke, T.R., 2002. *Boundary Layer Climates*. Routledge.
- Owen, S.M., Sieg, C.H., Fule, P.Z., Gehring, C.A., Baggett, L.S., Iniguez, J.M., Fornwalt, P.J., Battaglia, M.A., 2020. Persistent effects of fire severity on ponderosa pine regeneration niches and seedling growth. *Forests Ecology and Management*. 477, 118502. <https://doi.org/10.1016/j.foreco.2020.118502>
- Pierce, K.B., Lookingbill, T., Urban, D., 2005. A simple method for estimating potential relative radiation (PRR) for landscape-scale vegetation analysis. *Landscape Ecology* 20(2), 137–147. <https://doi.org/10.1007/s10980-004-1296-6>
- Pincebourde, S., Salle, A., 2020. On the importance of getting fine-scale temperature records near any surface. *Global Change Biology* 26(11), 6025–6027. <https://doi.org/10.1111/gcb.15210>
- Prévosto, B., Helluy, M., Gavinet, J., Fernandez, C., Balandier, P., 2020. Microclimate in Mediterranean pine forests: What is the influence of the shrub layer? *Agricultural and Forest Meteorology* 282–283, 107856. <https://doi.org/10.1016/j.agrformet.2019.107856>
- Qi, W., Saarela, S., Armston, J., Ståhl, G., Dubayah, R., 2019. Forest biomass estimation over three distinct forest types using TanDEM-X InSAR data and simulated GEDI lidar data. *Remote Sensing of Environment* 232, 111283. <https://doi.org/10.1016/j.rse.2019.111283>
- R Core Team, 2019. R Foundation for Statistical Computing. R: A language and environment for statistical computing.
- Reed, D.E., Ewers, B.E., Pendall, E., Frank, J., Kelly, R., 2018. Bark beetle-induced tree mortality alters stand energy budgets due to water budget changes. *Theoretical Applied Climatology* 131(1), 153–165. <https://doi.org/10.1007/s00704-016-1965-9>
- Refsland, T., Fraterrigo, J., 2018. Fire increases drought vulnerability of *Quercus alba* juveniles by altering forest microclimate and nitrogen availability. *Functional Ecology* 32(10), 2298–2309. <https://doi.org/10.1111/1365-2435.13193>
- Rodriguez-Iturbe, I., D’Odorico, P., Porporato, A., Ridolfi, L., 1999. On the spatial and temporal links between vegetation, climate, and soil moisture. *Water Resources Research* 35(12), 3709–3722. <https://doi.org/10.1029/1999WR900255>
- Roussel, J.-R., Auty, D., De Boissieu, F., Meador, A.S., 2021. package “lidR”: Airborne LiDAR data manipulation and visualization for forestry applications."
- Rutter, A.J., Kershaw, K.A., Robins, P.C., Morton, A.J., 1971. A predictive model of rainfall interception in forests: Derivation of the model from observations in a plantation of Corsican pine. *Agricultural Meteorology* 9, 367–384. [https://doi.org/10.1016/0002-1571\(71\)90034-3](https://doi.org/10.1016/0002-1571(71)90034-3)
- Salamí, E., Barrado, C., Pastor, E., 2014. UAV flight experiments applied to the remote sensing of vegetated areas. *Remote Sensing* 6(11), 11051–11081. <https://doi.org/10.3390/rs6111051>
- Scheiner, S.M., Gurevitch, J. (Eds.), 2001. *Design and analysis of ecological experiments*, 2nd ed. Oxford University Press, Oxford ; New York.
- Seidl, R., Thom, D., Kautz, M., Martin-Benito, D., Peltoniemi, M., Vacchiano, G., Wild, J., Ascoli, D., Petr, M., Honkaniemi, J., Lexer, M.J., Trotsiuk, V., Mairota, P., Svoboda, M., Fabrika, M., Nagel, T.A., Reyer, C.P.O., 2017. Forest disturbances under climate change. *Nature Climate Change* 7(6), 395–402. <https://doi.org/10.1038/nclimate3303>

- Stevens-Rumann, C.S., Kemp, K.B., Higuera, P.E., Harvey, B.J., Rother, M.T., Donato, D.C., Morgan, P., Veblen, T.T., 2018. Evidence for declining forest resilience to wildfires under climate change. *Ecology Letters* 21(2), 243–252. <https://doi.org/10.1111/ele.12889>
- Talucci, A.C., Forbath, E., Kropp, H., Alexander, H.D., DeMarco, J., Paulson, A.K., Zimov, N.S., Zimov, S., Loranty, M.M., 2020. Evaluating post-fire vegetation recovery in Cajander larch forests in northeastern Siberia using UAV derived vegetation indices. *Remote Sensing* 12(18), 2970. <https://doi.org/10.3390/rs12182970>
- Talucci, A.C., Lertzman, K.P., Krawchuk, M.A., 2019. Drivers of lodgepole pine recruitment across a gradient of bark beetle outbreak and wildfire in British Columbia. *Forest Ecology and Management* 451, 117500. <https://doi.org/10.1016/j.foreco.2019.117500>
- Thom, D., Rammer, W., Seidl, R., 2017. The impact of future forest dynamics on climate: interactive effects of changing vegetation and disturbance regimes. *Ecological Monographs* 87(4), 665–684. <https://doi.org/10.1002/ecm.1272>
- Thom, D., Sommerfeld, A., Sebald, J., Hagge, J., Müller, J., Seidl, R., 2020. Effects of disturbance patterns and deadwood on the microclimate in European beech forests. *Agricultural and Forest Meteorology* 291, 108066. <https://doi.org/10.1016/j.agrformet.2020.108066>
- Tomaščík, J., Mokroš, M., Saloň, Š., Chudý, F., Tunák, D., 2017. Accuracy of photogrammetric UAV-based point clouds under conditions of partially-open forest canopy. *Forests* 8(5), 151. <https://doi.org/10.3390/f8050151>
- Tompalski, P., Rakofsky, J., Coops, N.C., White, J.C., Graham, A.N.V., Rosychuk, K., 2019. Challenges of multi-temporal and multi-sensor forest growth analyses in a highly disturbed boreal mixedwood forests. *Remote Sensing* 11(18), 2102. <https://doi.org/10.3390/rs11182102>
- Vanwalleghe, T., Meentemeyer, R.K., 2009. Predicting forest microclimate in heterogeneous landscapes. *Ecosystems* 12(7), 1158–1172. <https://doi.org/10.1007/s10021-009-9281-1>
- Varner, J., Dearing, M.D., 2014. The importance of biologically relevant microclimates in habitat suitability assessments. *PLoS One* 9(8), e104648. <https://doi.org/10.1371/journal.pone.0104648>
- Vauhkonen, J., Ene, L., Gupta, S., Heinzl, J., Holmgren, J., Pitkänen, J., Solberg, S., Wang, Y., Weinacker, H., Hauglin, K.M., Lien, V., Packalén, P., Gobakken, T., Koch, B., Næsset, E., Tokola, T., Maltamo, M., 2012. Comparative testing of single-tree detection algorithms under different types of forest. *Forestry* 85(1), 27–40. <https://doi.org/10.1093/forestry/cpr051>
- von Arx, G., Dobbertin, M., Rebetez, M., 2012. Spatio-temporal effects of forest canopy on understory microclimate in a long-term experiment in Switzerland. *Agricultural and Forest Meteorology* 166–167, 144–155. <https://doi.org/10.1016/j.agrformet.2012.07.018>
- von Arx, G., Pannatier, E.G., Thimonier, A., Rebetez, M., 2013. Microclimate in forests with varying leaf area index and soil moisture: potential implications for seedling establishment in a changing climate. *Journal of Ecology* 101(5), 1201–1213. <https://doi.org/10.1111/1365-2745.12121>
- von Haden, A.C., Marín-Spiotta, E., Jackson, R.D., Kucharik, C.J., 2019. Soil microclimates influence annual carbon loss via heterotrophic soil respiration in maize and switchgrass bioenergy cropping systems. *Agricultural and Forest Meteorology* 279, 107731. <https://doi.org/10.1016/j.agrformet.2019.107731>

- Wallace, L., Lucieer, A., Malenovský, Z., Turner, D., Vopěnka, P., 2016. Assessment of forest structure using two UAV techniques: A comparison of airborne laser scanning and structure from motion (SfM) point clouds. *Forests* 7(3), 62. <https://doi.org/10.3390/f7030062>
- Westerling, A.L., Hidalgo, H.G., Cayan, D.R., Swetnam, T.W., 2006. Warming and earlier spring increase western U.S. forest wildfire activity. *Science* 313(5789), 940–943. <https://doi.org/10.1126/science.1128834>
- White, J.C., Tompalski, P., Coops, N.C., Wulder, M.A., 2018. Comparison of airborne laser scanning and digital stereo imagery for characterizing forest canopy gaps in coastal temperate rainforests. *Remote Sensing of Environment* 208, 1–14. <https://doi.org/10.1016/j.rse.2018.02.002>
- Wild, J., Kopecký, M., Macek, M., Šanda, M., Jankovec, J., Haase, T., 2019. Climate at ecologically relevant scales: A new temperature and soil moisture logger for long-term microclimate measurement. *Agricultural and Forest Meteorology* 268, 40–47. <https://doi.org/10.1016/j.agrformet.2018.12.018>
- Williams, A.P., Allen, C.D., Macalady, A.K., Griffin, D., Woodhouse, C.A., Meko, D.M., Swetnam, T.W., Rauscher, S.A., Seager, R., Grissino-Mayer, H.D., Dean, J.S., Cook, E.R., Gangodagamage, C., Cai, M., McDowell, N.G., 2013. Temperature as a potent driver of regional forest drought stress and tree mortality. *Nature Climate Change* 3(3), 292–297. <https://doi.org/10.1038/nclimate1693>
- Zellweger, F., De Frenne, P., Lenoir, J., Rocchini, D., Coomes, D., 2019. Advances in microclimate ecology arising from remote sensing. *Trends in Ecology & Evolution* 34(4), 327–341. <https://doi.org/10.1016/j.tree.2018.12.012>
- Zellweger, F., Frenne, P.D., Lenoir, J., Vangansbeke, P., Verheyen, K., Bernhardt-Römermann, M., Baeten, L., Hédl, R., Berki, I., Brunet, J., Calster, H.V., Chudomelová, M., Decocq, G., Dirnböck, T., Durak, T., Heinken, T., Jaroszewicz, B., Kopecký, M., Máliš, F., Macek, M., Malicki, M., Naaf, T., Nagel, T.A., Ortmann-Ajkai, A., Petřík, P., Pielech, R., Reczyńska, K., Schmidt, W., Standovár, T., Świerkosz, K., Teleki, B., Vild, O., Wulf, M., Coomes, D., 2020. Forest microclimate dynamics drive plant responses to warming. *Science* 368 (6492), 772–775. <https://doi.org/10.1126/science.aba6880>
- Zhu, D., Ciais, P., Krinner, G., Maignan, F., Jornet Puig, A., Hugelius, G., 2019. Controls of soil organic matter on soil thermal dynamics in the northern high latitudes. *Nature Communications* 10(1), 1–9. <https://doi.org/10.1038/s41467-019-11103-1>

Appendices

Appendix A RPA flights and 3D point cloud development

Table S1 Details of equipment and flight planning for RPA image acquisition.

Aircraft	
Max Flight Time	Approximately 30 mins
Navigation	RTK
GPS Positional Accuracy	Vert. +/-0.1; Horizontal, +/- 0.1 m
Transmission Range	7 km
Camera	
Sensor	1" CMOS
ISO Range	100-3200
Electronic Shutter Speed	1/8000 s
FOV	84 °
Aperture	f/2.8
Image Size	4864 x 3648
Acquisition Parameters	
Altitude	70 m (AGL)
Terrain Following	15 m (ALS)
Image Overlap	90 % forward, 80% lateral

Table S2 Point cloud accuracy for photo-alignment (RTK photo alignment), LiDAR ICP alignment and orthophoto rectification

Flight Area	High	Middle	Low	Old Growth
RTK Photo Alignment (m)	0.21	0.19	0.0082	0.14
# of Tie-Points	1,150,051	509,158	1,589,590	1,129,400
LiDAR-Point Cloud ICP Alignment (m)	1.83	1.86	1.58	0.90
Canopy Height – Orthophoto Alignment (m)	0.28	2.26	0.97	0.70

Appendix B Microclimate data cleaning

B.1 Rolling mean standard deviation in soil temperature

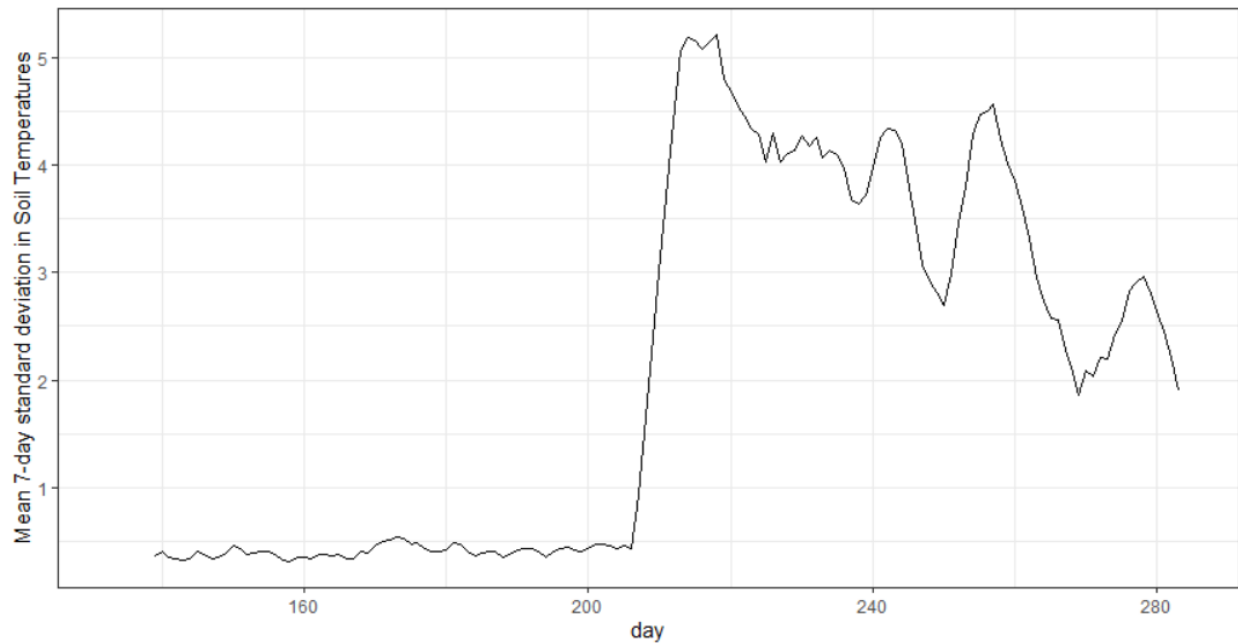


Figure S1 Example from datalogger 66 of the 7-day mean of soil temperature daily standard deviation used to clip data. A large increase in the 7-day mean supports the datalogger 66 was removed on day 204.

B.2 Microclimate data included in analyses

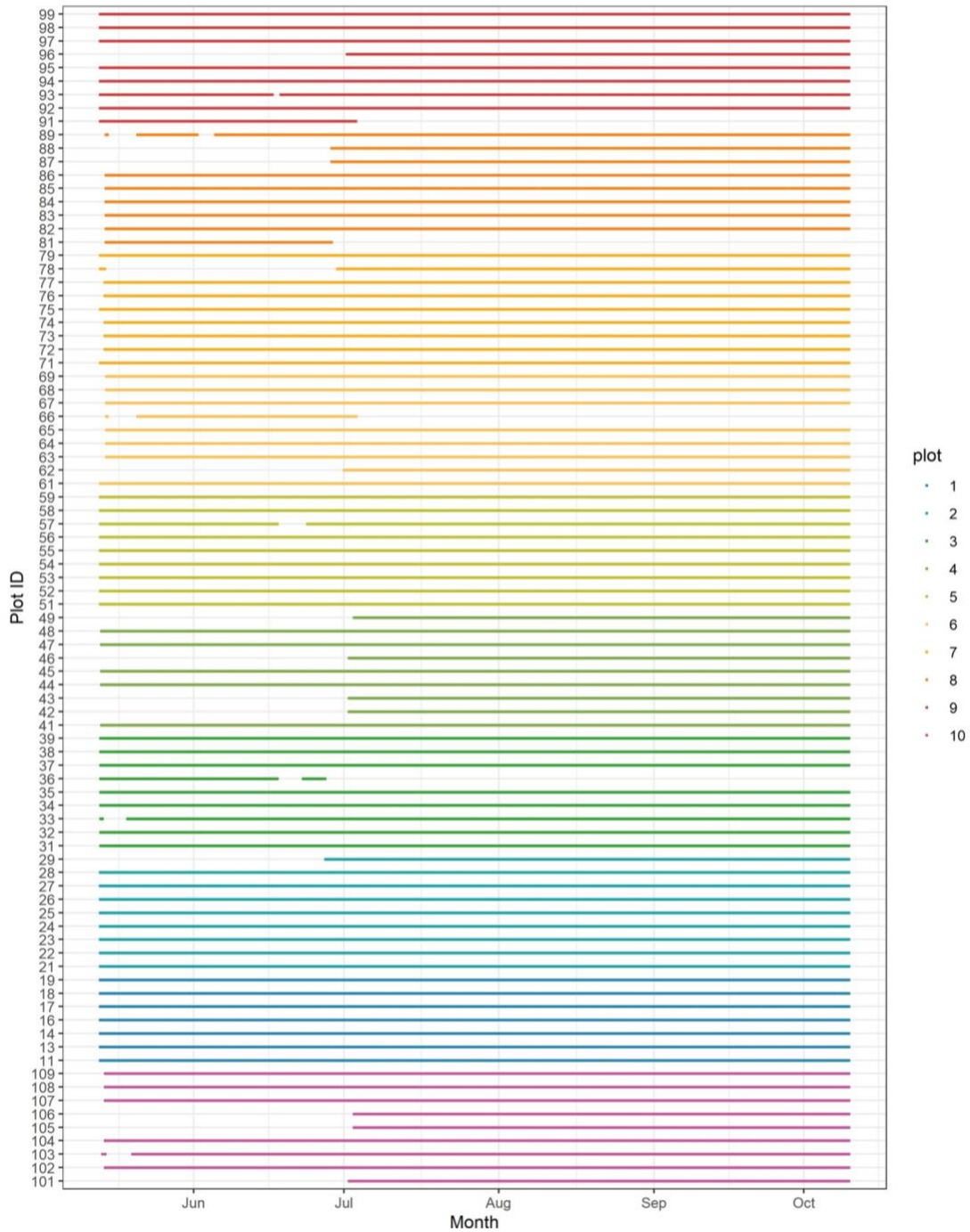


Figure S2 Soil Moisture, soil and surface temperatures included in analyses. Plot ID is noted on the vertical axis, and lines are colored by forest plot. Data were removed based on known issues with the data (the logger was pulled out of the ground) or erroneous data (unusually high or low values).

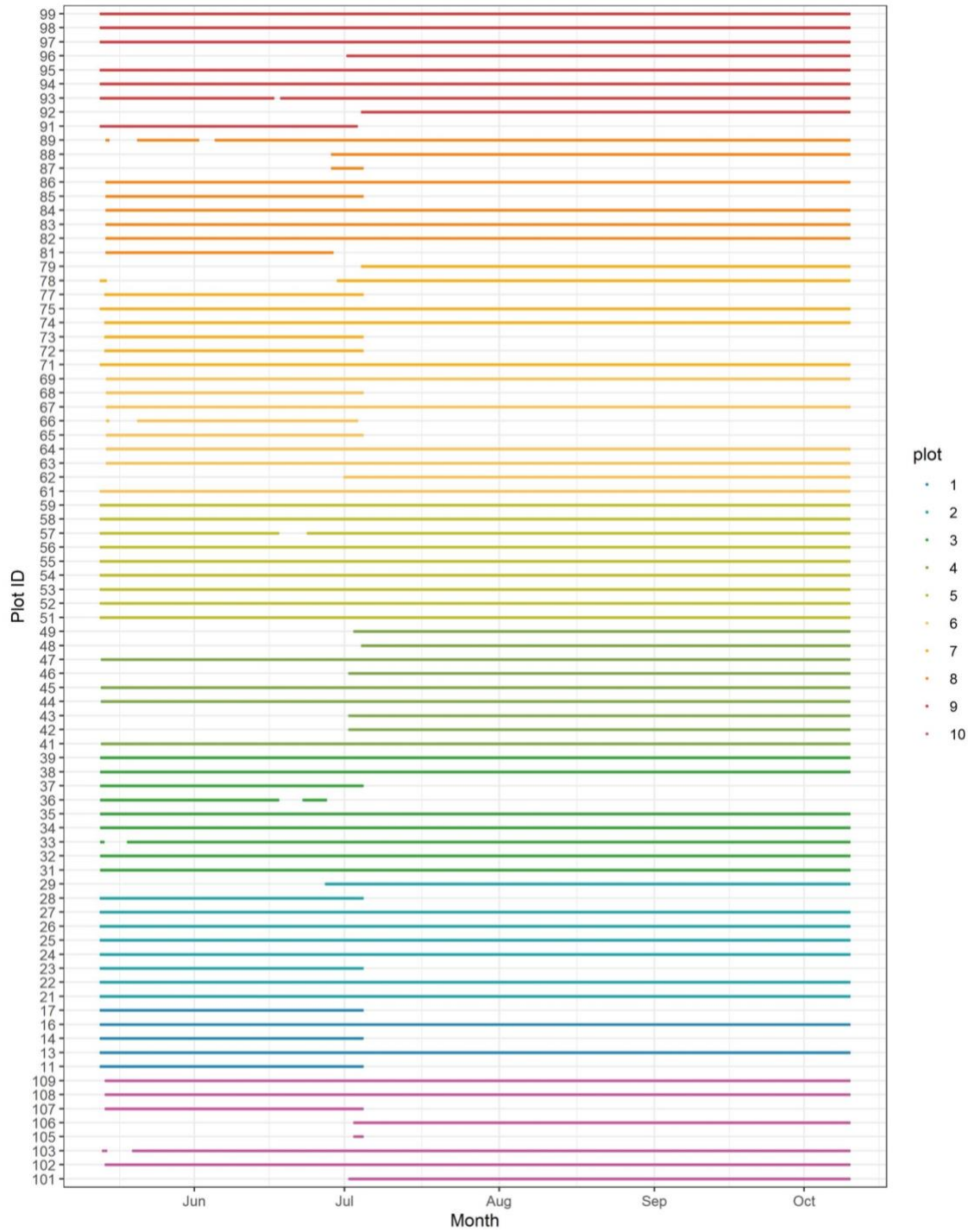


Figure S3 Near-Surface temperatures included in analyses. Plot ID is noted on the vertical axis, and lines are colored by forest plot. Data were removed based on known issues with the data (the solar shield was removed) or the data were erroneous (unusually high or low values).

Appendix C Canopy height models and verification

C.1 Canopy height models

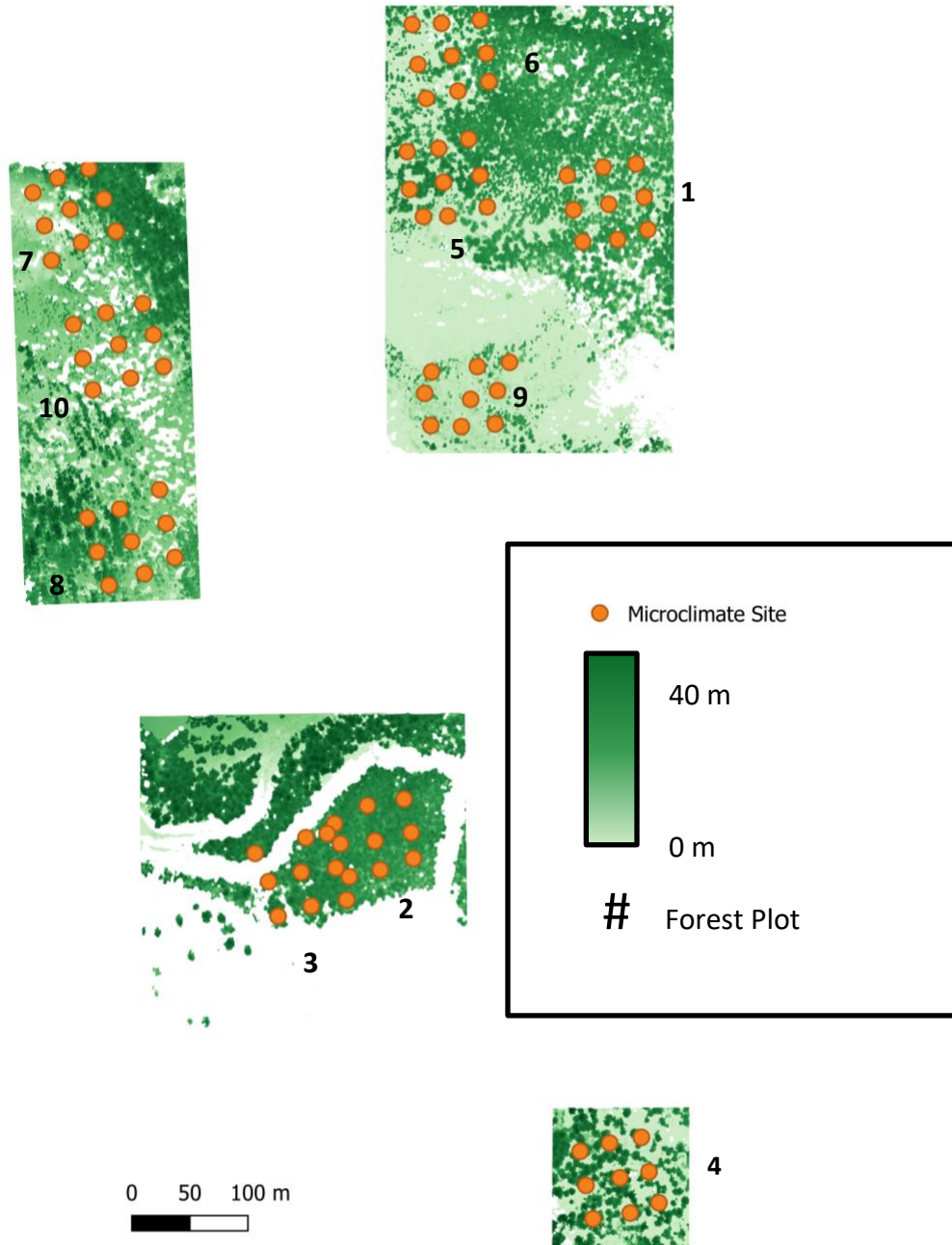


Figure S4 Canopy height models for the field site. Each raster has a 10cm resolution, and the color scale is the same for all plots. Datalogger locations are noted in orange. Numbers are the plot locations.

C.2 Canopy verification plots

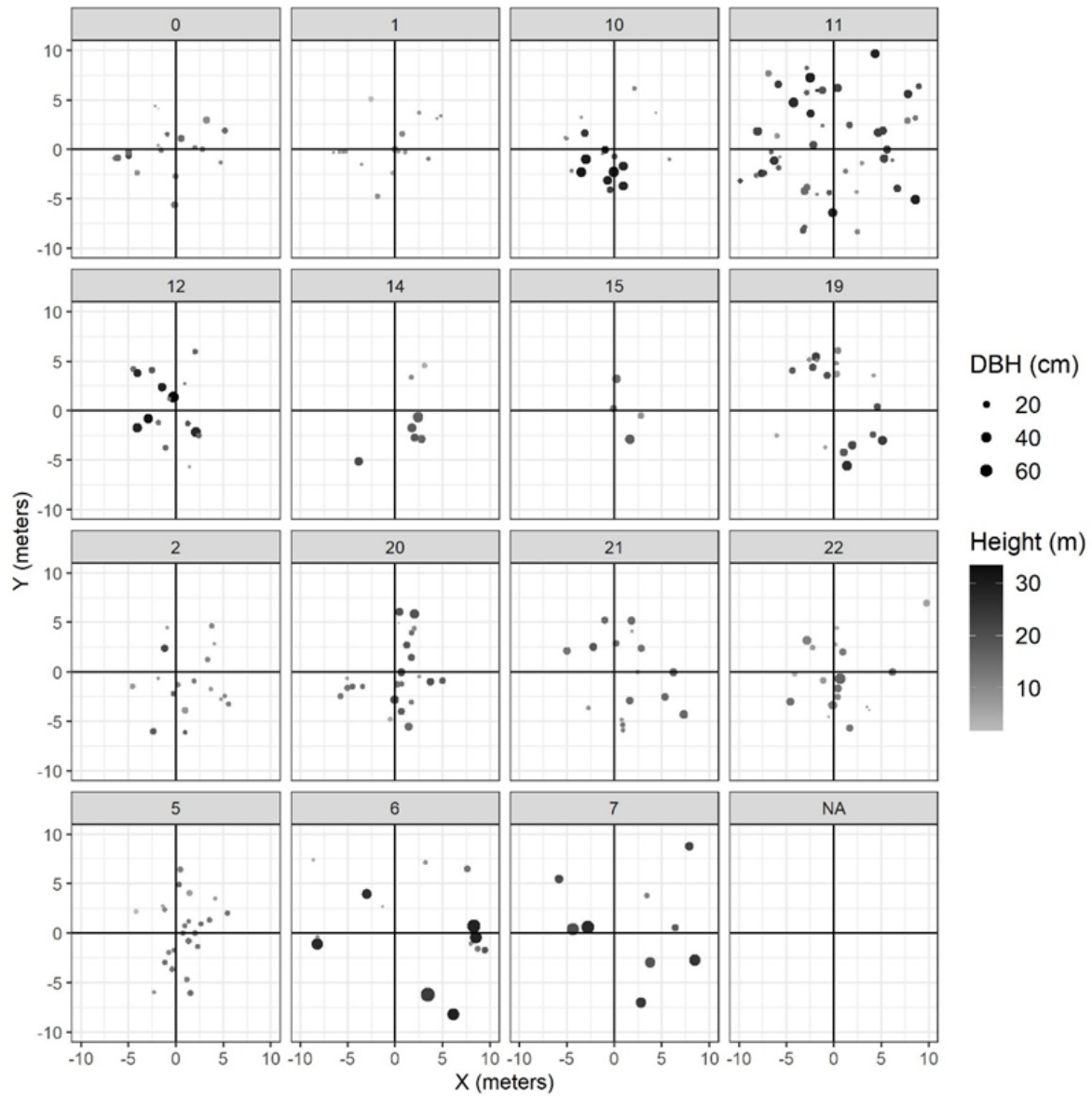


Figure S5 Verification plots for canopy height models. Plots are labeled according to randomly assigned labels. Points are the distance from plot center. Tree height (m) is a gray scale of white to black and point size corresponds to diameter-at-breast-height (cm).

C.3 Accuracy of DAP model compared to field measured sites

To verify my canopy height model, I randomly selected 15 6.5 m radius verification plots from the Alex Fraser Research Forest Field Site (Figure 3.1). Across all canopy verification plots, a total of 295 stems (live and dead) were measured with a range of 2 to 27 and an average of 18 stems per verification plot. We recorded tree height (m), diameter at breast height (cm), tree status (alive vs. dead), and crown class (dominant, co-dominant, intermediate, and suppressed). Tree height was recorded using a Nikon Forester 550 Hypsometer. To ensure accurate heights, we took the mean of three measurements of tree height from different positions. I used simple linear models to compare the mean verification plot height measured in the field to those produced by the RPA imagery. Models comparing DAP derived and field-measured canopy heights had strong alignment for both mean ($R^2 = 0.7$) and max ($R^2 = 0.46$) canopy height (Figure S11). DAP height measurements were significant predictors of field height measurements ($p < 0.05$ for maximum and mean height). DAP did not overestimate maximum height ($p > 0.05$ for model intercepts). However, DAP measurements overpredicted mean canopy height ($p < 0.05$, intercept = 6.61 m). I removed one verification plot from the model, which was dominated by sub-canopy trees. This decreased the overprediction of DAP heights by 1.3 m ($p < 0.05$, intercept = 5.34).

I acknowledge that the canopy height model overestimated low canopy height values. This is likely due to the inclusion of dead and sub-canopy trees that are difficult to capture in DAP modeling. Additionally, because we compare a raster of canopy height to field measurements of trees, the accuracy of the model varies as a function of tree form. In Figure S11, three plots with the lowest estimated DAP mean height were in areas that experienced a crown fire. The DAP raster captured the tallest tree height, but as we averaged over a 6.5 radius,

the lack of a tree crown skewed the DAP model to overpredicted tree height (many of the pixels had low height values because trees had no crown). When points in crown fire and the point with a dominance of sub-canopy trees were removed, the model fit was improved ($R^2 = 0.82$) and fit a one-to-one line (model not depicted, slope = 1.0 $p \ll 0.05$, intercept = 0.1 $p > 0.5$). Thus, my DAP-derived heights may better represent the ultimate impact on microclimate because they better describe the form of tree crowns.

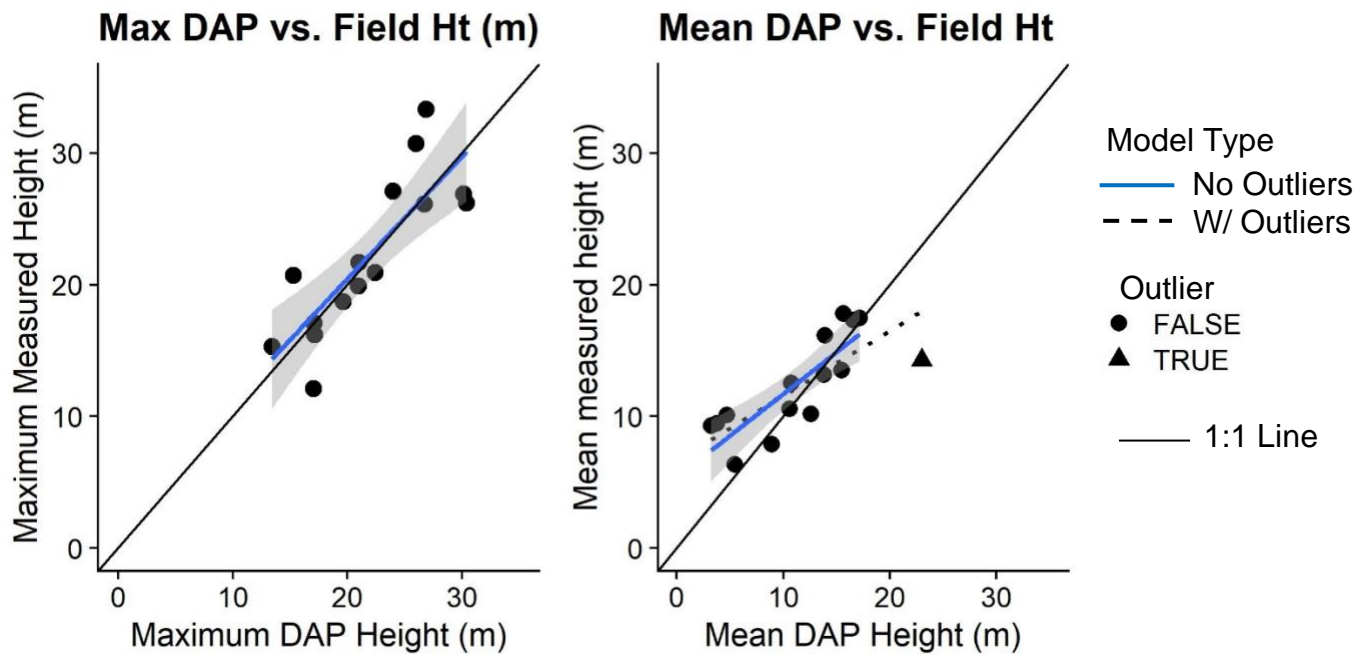


Figure S6 Comparison of DAP derived and field measured maximum and mean verification plot heights. The dotted line in S11B is the model result including the outlier data point (the triangle).

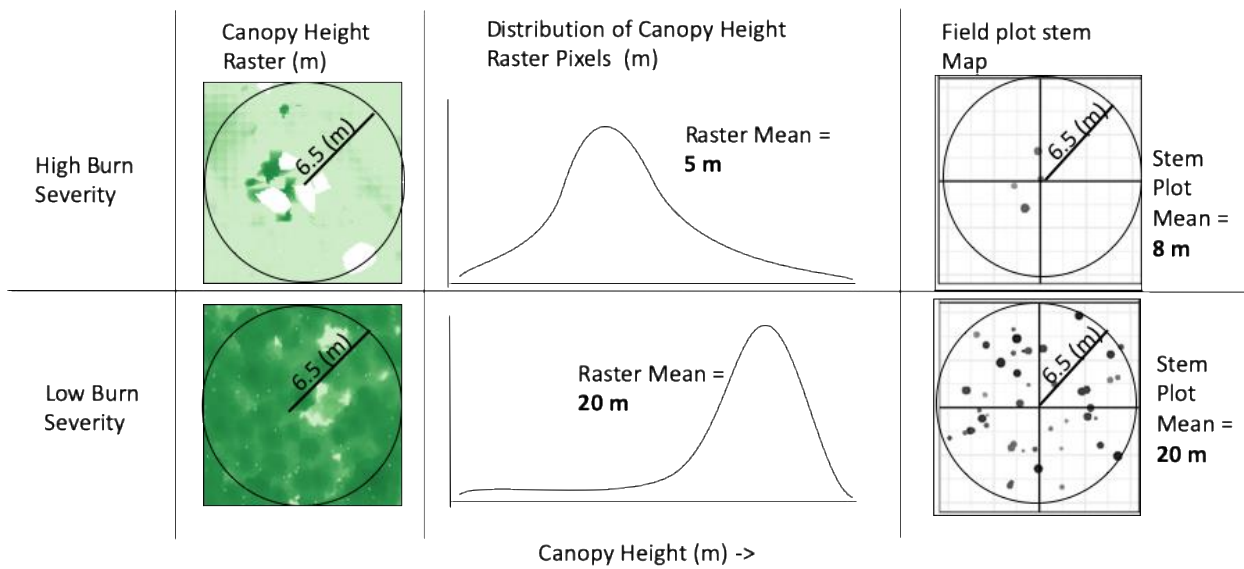


Figure S7 Description of error introduced comparing high burn severity canopy height data to low burn severity canopy height data. Circles denote the plot area. Stem plot circles depict diameter-at-breast-height (cm) of measured stems. Height values are arbitrarily chosen to show differences in high and low burn severity canopy height rasters and field plot data.

Appendix D Correlation coefficients for canopy attributes and model predictors

D.1 Correlation between canopy height and canopy cover

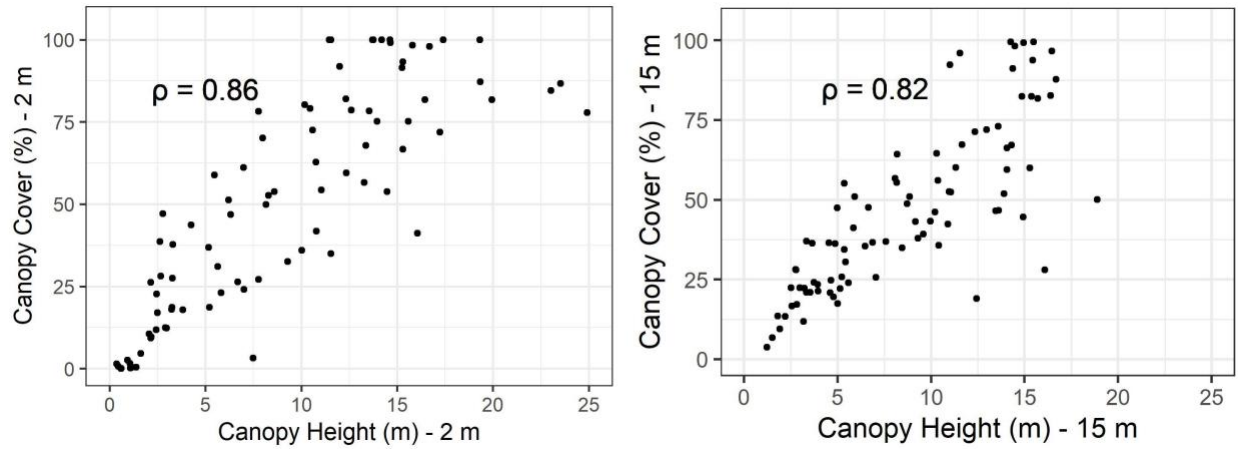


Figure S8 Correlation between canopy cover and canopy height for radii used in microclimate modeling.

Rho (ρ) is the spearman correlation of the two variables

D.2 Correlation between model fixed effects

Table S3 Pearson's correlation coefficient for fixed effects used in mixed linear models. Correlation coefficients are included for canopy calculated at the 2 m (used to model soil moisture) and 15 m (used to model soil temperature) radius.

Fixed Effects	Pearson's Correlation Coefficient
Canopy Height (15m radius) ~ Aspect	-0.094
Canopy Height (2 m radius) ~ Elevation	-0.10
Canopy Height (15m radius) ~ Elevation	-0.50
Canopy Height (2 m radius) ~ Aspect	-0.35
Elevation ~Aspect	0.12

Appendix E Estimated parameters of monthly models for all explanatory variables

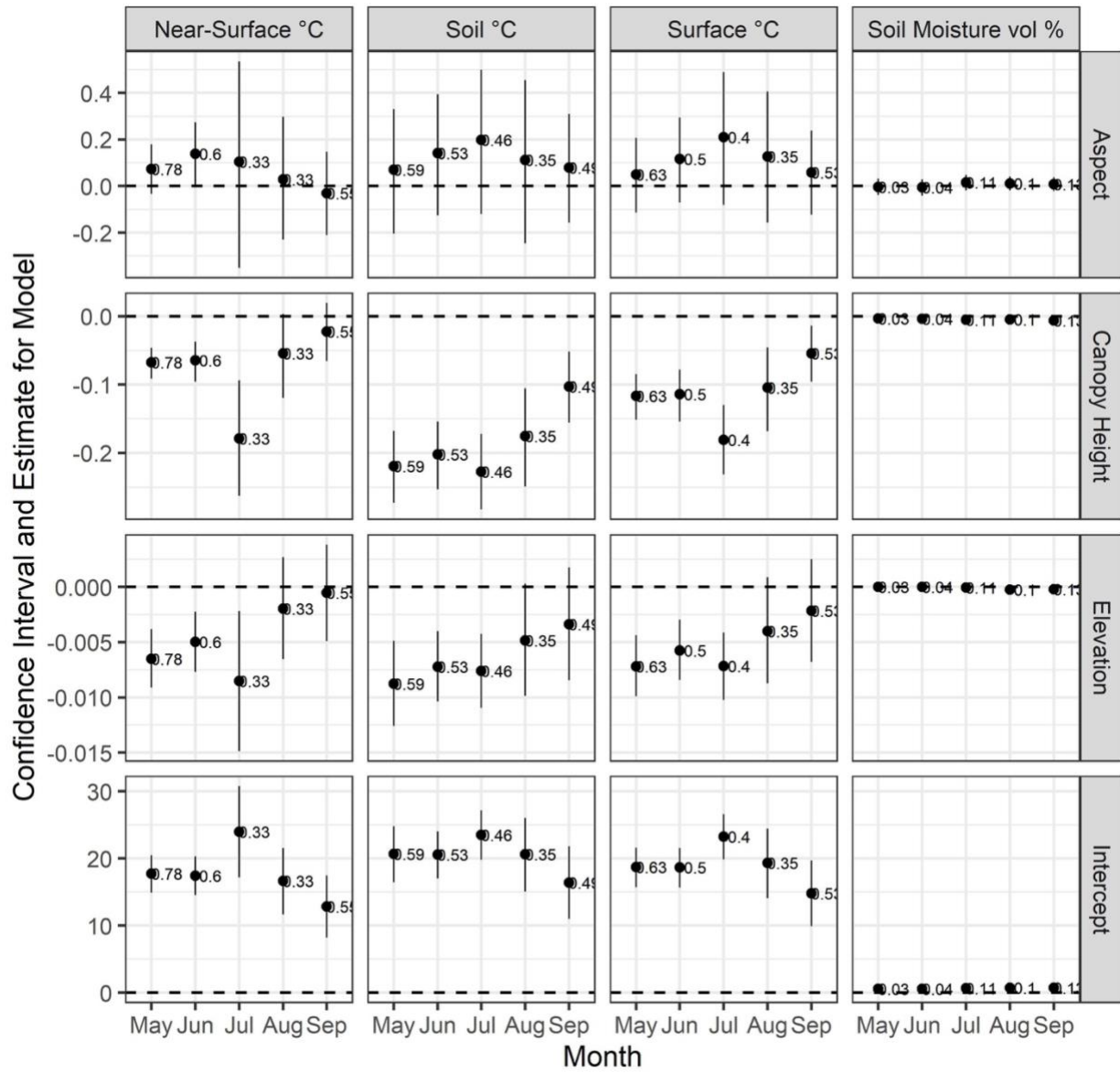


Figure S9 Estimated parameter for fixed effects on mean microclimate variables averaged by month (Near-Surface, Soil, Surface, and Soil Moisture vol %). Points show estimated parameters, and surrounding lines are the 95% confidence intervals for parameters. Printed text values are the adjusted model R². Note: vertical scales differ among panels.

Appendix F Field collected data

F.1 Vegetation and leaf litter data

Five measurements of vegetation height and litter depth were randomly collected and values averaged for each site-location. Dominant cover was estimated based on percentages between 0-5, 5-10, 10-25, 25-50, 50-75, and 75-100 %. Cover classes included: shrub, herbs, forbs, graminoids, moss, or bare. Litter and vegetation heights are noted in Figure S4.

We also collected seedling data. At points 2, 4,5,6, and 8 within each logger set up we took one seedling plot. We recorded total number according to three morphologies (A, B, C). A is a Douglas-fir seedling, B is a lodgepole pine, and C is spruce. These are recorded under "morpho" of the vegetation data.

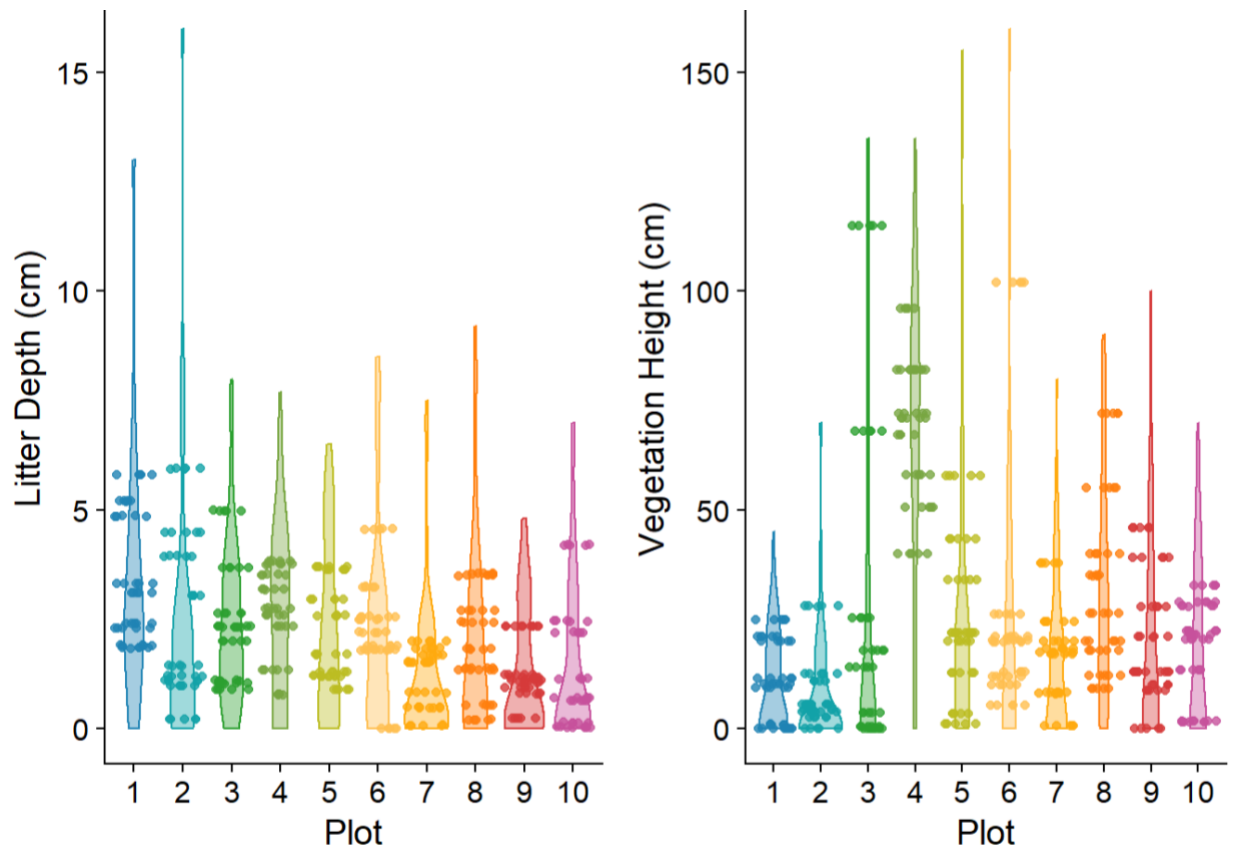


Figure S10 Variability in litter depth and vegetation height. Points are average values for each datalogger. Distribution is based on all points (5 per datalogger).

F.2 Soil data

For each datalogger 3-5 soil cores were collected using a standard push soil sample probe at depths of 15 to 30 cm. An example of a soil core is shown in Figure S5. The volume, depth and number of soil samples varied from location-to-location based on the presence of large clasts (see Figure S6 for examples). Soil samples were dried over a one-week period at 45 °C in a standard drying oven. I calculated soil bulk density based on the volume of soil collected and the final dry weight. Variation in soil bulk density is noted in Figure S7. Soil type was classified using the standard soil classification based on percent silt, clay, and sand. Samples with high organic content were noted, but organic material was not digested. Soil composition was used to

convert soil moisture counts into volumetric soil moisture (% vol) using the "TMS3_Calibr User Soil Properties" function. The function applies a conversion factor with three different coefficients, a, b, and c, and equation S1 where X is the soil moisture count.

$$f(x) = ax^2 + bx + c \quad \text{S1}$$



Figure S11 Example soil core from plot six datalogger number four. Soil cores generally showed these three distinct layers, organic dominant (top), silty sand matrix (middle), and a silt matrix (base).



Figure S12 Soil samples from plot 4. Samples are combined cores from each datalogger.

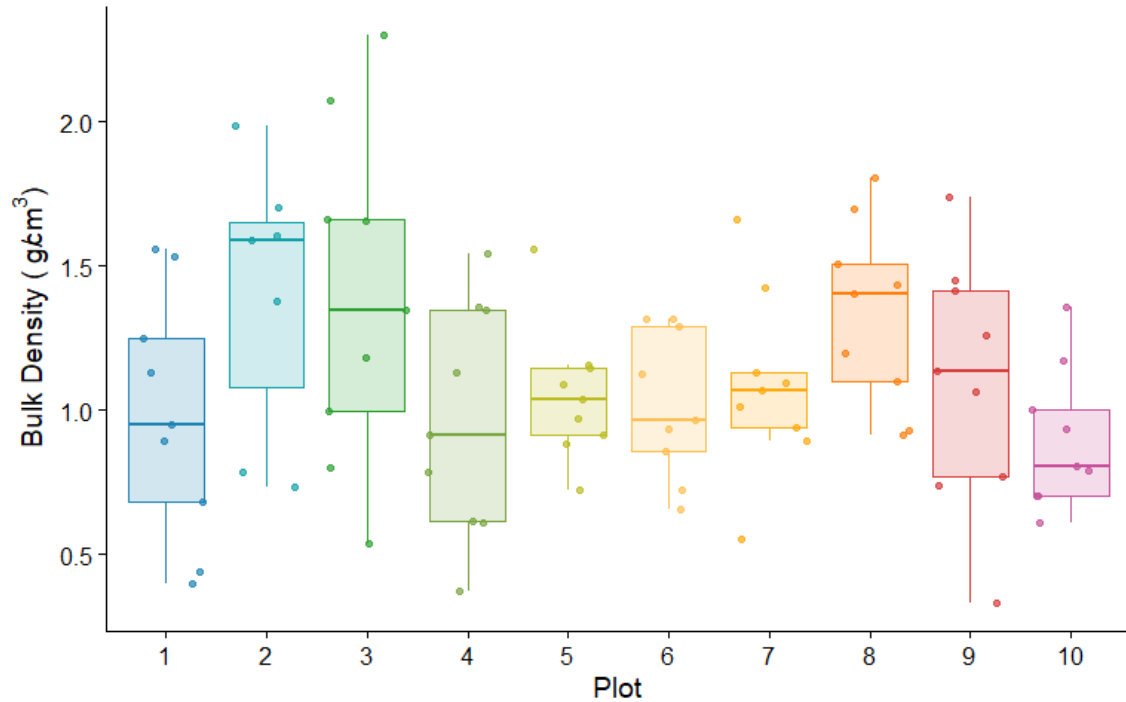


Figure S13 Plot-level variability in bulk density (g/cm^3). Points show values derived for each plot

F.3 Leaf area index data

LAI was measured using a Licor 2200 Plant Canopy Analyzer. The Licor 2220 is a passive sensor of leaf area index that combines measurements of solar radiation taken at five concentric circles with angles centered at 7° , 23° , 38° , 53° , 68° relative to vertical. Values of LAI are calculated from the difference of measured radiation below canopy and measurements from nearby non-canopy locations (also known as the above measurement). At each datalogger, four measurements were taken at a 2 m distance from the logger in ordinal directions. These measurements were averaged to produce an LAI for each location. In some cases, the references non-canopy location failed to record; the associated below measurements have been removed from the data.

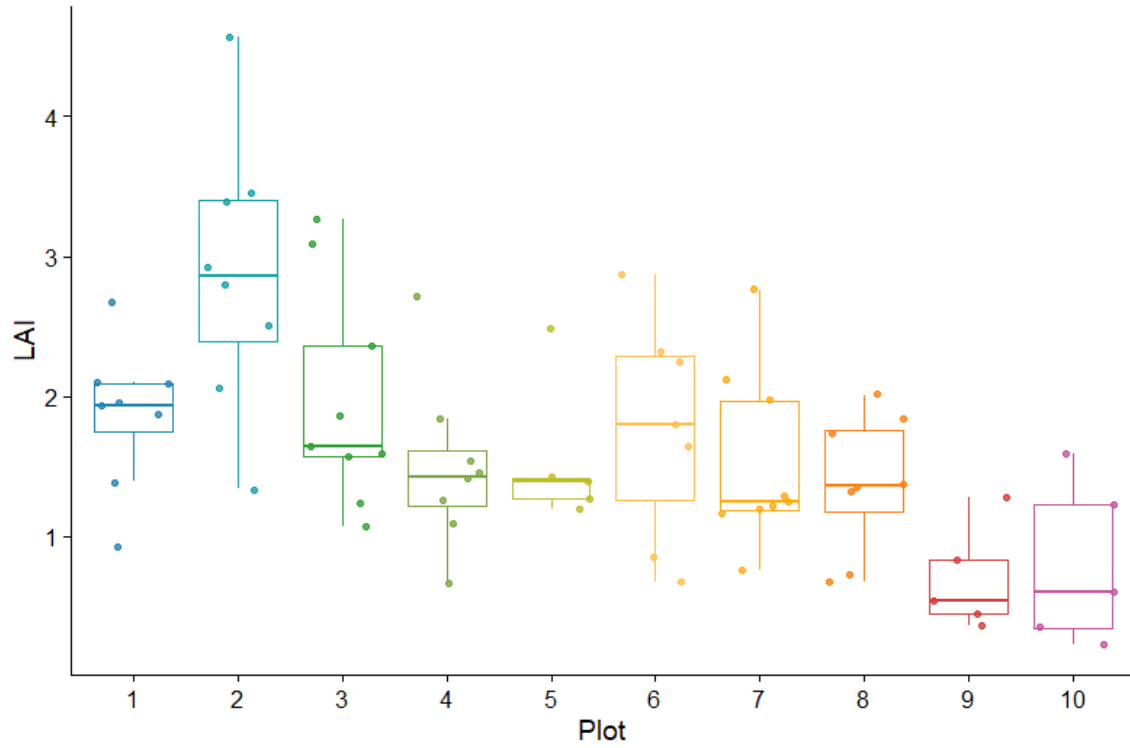


Figure S14 Leaf area index measurements for each datalogger. Points and boxes are colored by plot number.